IEEE Access
Multidisciplinary | Rapid Review | Open Access Journal

Received January 27, 2022, accepted February 13, 2022, date of publication February 16, 2022, date of current version March 1, 2022.

Digital Object Identifier 10.1109/ACCESS.2022.3152160

Modified Interactive Algorithm Based on Runge Kutta Optimizer for Photovoltaic Modeling: Justification Under Partial Shading and Varied Temperature Conditions

DALIA YOUSRI[1], MOHAMMED MUDHSH[2], YOMNA O. SHAKER[1,3], LAITH ABUALIGAH[4,5], ELSAYED TAG-ELDIN[6], MOHAMED ABD ELAZIZ[7,8,9,10], AND DALIA ALLAM[1]

[1]Department of Electrical Engineering, Faculty of Engineering, Fayoum University, Fayoum 63514, Egypt
[2]School of Information Engineering, Henan Institute of Science and Technology, Xinxiang 453003, China
[3]Engineering Department, University of Science and Technology of Fujairah (USTF), Fujairah, United Arab Emirates
[4]Faculty of Computer Sciences and Informatics, Amman Arab University, Amman 11953, Jordan
[5]School of Computer Sciences, Universiti Sains Malaysia, Pulau Pinang 11800, Malaysia
[6]Electrical Engineering Department, Faculty of Engineering and Technology, Future University in Egypt, Cairo 11835, Egypt
[7]Faculty of Computer Science and Engineering, Galala University, Suez 435611, Egypt
[8]Artificial Intelligence Research Center (AIRC), Ajman University, Ajman, United Arab Emirates
[9]Department of Mathematics, Faculty of Science, Zagazig University, Zagazig 44519, Egypt
[10]School of Computer Science and Robotics, Tomsk Polytechnic University, 634050 Tomsk, Russia

Corresponding author: Elsayed Tag-Eldin (elsayed.tageldin@fue.edu.eg)

ABSTRACT The accuracy of characteristic the PV cell/module/array under several operating conditions of radiation and temperature mainly relies on their equivalent circuits sequentially; it is based on identified parameters of the circuits. Therefore, this paper proposes a modified interactive variant of the recent optimization algorithm of the rung-kutta method (MRUN) to determine the reliable parameters of single and double diode models parameters for different PV cells/modules. The results of the MRUN optimizer are validated via series of statistical analyses compared with five new meta-heuristic algorithms including aquila optimizer (AO), electric fish optimizer (EFO), barnacles mating optimizer (BMO), capuchin search algorithm (CapSA), and red fox optimization algorithm (RFSO) moreover, twenty-five state-of the art techniques from literature. Furthermore, the identified parameters certainty is evaluated in implementing the characteristics of an entire system consists of series (S), and series-parallel (S-P) PV arrays with numerous dimensions. The considered arrays dimensions are three series (3S), six series (6S), and nine series (9S) PV modules. For the investigated arrays, three-dimensional arrays are recognized. The first array comprises 3S-2P PV modules where two parallel strings (2P) have three series modules in each string (3S). The second array consists of six series-three parallel (6S-3P) PV modules, and the third one has nine series-nine parallel (9S-9P) PV modules. The results prove that the proposed algorithm precisely and reliably defines the parameters of different PV models with root mean square error and standard deviation of $7.7301e^{-4} \pm 4.9299e^{-6}$, and $7.4653e^{-4} \pm 7.2905e^{-5}$ for 1D, and 2D models, respectively meanwhile the RUN have $7.7438e^{-4} \pm 3.5798e^{-4}$, and $7.5861e^{-4} \pm 4.1096e^{-4}$, respectively. Furthermore MRUN provided extremely competing results compared to other well-known PV parameters extraction methods statistically as it has.

INDEX TERMS Double diode PV model, partial shading, single diode PV model, PV parameters estimation, rung-kutta optimizer, series-parallel array.

NOMENCLATURE

ACRONYMS

NOCT	Nominal operating cell temperature.
PS	Partial shading.
RMSE	root mean square error.

CONSTANTS

Cf_i	Temperature coefficient of current.
q	Charge of electron 1.6×10^{-19} C.
k	Boltzmann constant $1.35 \times 10^{-23} J/K$.
k_v	Temperature coefficient of voltage.
k_p	Temperature coefficient of maximum power.

The associate editor coordinating the review of this manuscript and approving it for publication was Hao Wang.

VARIABLES

E_g	Band-gap energy.
R_{sh}	Shunt resistance (Ω).
$\vec{Z}$	Vector of the identified parameters.
$a_{1,2}$	Ideality factors.
I	Solar cell output current (A).
I_p	Leakage shunt currents (A).
I_{array}	Array current (A).
$I_{d1,2}$	Diodes currents (A).
I_{est}	Estimated current (A).
$I_{Lambert}$	Calculated current via Lambert form.
I_{meas}	Measured current (A).
I_{mp}	Current at at maximum power point (MPP) (A).
$I_{o1,2}$	Diode reverse saturation currents.
$I_{SC_{Mi}}$	The module Mi short circuit current.
I_{str}	The current of string (A).
M	Length of the measured dataset.
N_s	Number of series cells.
P_{str}	String power.
R	The diode equivalent resistance in the conducing mode (Ω).
R_s	Series resistance (Ω).
T	Temperature of a PV cell in Kelvin.
$V_{Bypassdiode}$	The bypass diode voltage (V).
V_{fwd}	The diode forward voltage (V).
V_{mp}	Voltage at maximum power point (MPP) (V).
V_{oc}	Open circuit voltage (V).
V_{str}	Total voltage of string (V).
V_{th}	Thermal voltage.
I_{ph}	Photo-generated currents (A).
m	Number of modules in string.
n	Number of parallel strings in the array.
P_{max}	maximum power at SOC.

I. INTRODUCTION

Because of the rising and unstable prices of fossil fuels and pollution and solid wastes, renewable energy sources have emerged as a viable option for sustaining energy while reducing pollution [1]. Solar energy can be considered the most efficient alternative to fossil fuels and coal when power system operators meet energy needs. Solar energy is the most potential renewable energy source because of its global distribution, low maintenance, noise-free operation, and near-conventional production processes. Over the last three decades, efforts have been made to transition from small to large-scale solar cells or from cell size to module size [2]. This trend reflects advancements in solar cell technology, which have increased utilization levels from a small scale (few cells) to a big scale (many modules). Many limitations that previously limited its use in large-scale power system applications have now been removed.

Photovoltaic (PV) power is one of the preeminent universal renewable electricity methods behind wind power transforming methods worldwide [3]. Lately, active investments target the PV production outstandingly, and many revenues are advised to research in PV energy. Usually, such regulation arises from the severe cost reduction in the PV operation parts, which designates the enormous development of the PV industry [4], [5]. The cost of PV machines pointedly fell within the recent decade, including the PV operation itself with its design and adapters [6]. Thus, the PV price adjustment increases its defiance with other renewable energy operations. According to the statistics estimation budget of the universal requirement for PV operations, a fifty percent achievement rate of PV investments was returned with 306.5 GW in 2016 [7].

In this context, the PV system has gotten a lot of press in recent years [8], [9]. However, to examine the dynamic conversion behavior of a PV system, one must first understand how to model the PV cell, which is the system core component [10]. To represent PV cells, a variety of methodologies have been devised, the most prevalent of which is the use of comparable circuit models. The single diode and double diode types are the most often utilized circuit types [11]. The correctness of the parameters associated with the model structure is critical for estimating, sizing, performance assessment, management, efficiency computations, and reactive power control of solar PV systems after finding a suitable model structure [12].

Because of the nonlinear nature of photovoltaic models and the rising number of parameters that must be evaluated, metaheuristic approaches inspired by numerous natural phenomena have been widely employed to find parameters of PV models as a possible alternative to deterministic methodologies [13], [14]. Metaheuristic methods are employed to extract parameters with high precision. They do not put any constraints on the problem characteristics; therefore, they are simple to apply to a variety of real-world challenges [15]. The Grasshopper Optimization Algorithm (GOA) is used in [16] to extract parameters from a three-diode PV model. The simulation results are run at different temperatures and levels of irradiation. The GOA-based PV model efficiency is assessed by comparing its numerical findings to other optimization method-based PV models. A new optimization approach termed turbulent flow of water-based optimization is proposed in [17] to extract the characteristics of three photovoltaic (PV) cell models (TFWO). Compared to existing approaches, the suggested TFWO achieves a high degree of similarity between the estimated voltage-power (V-P) and current-voltage (I–V) curves. A gradient-based optimizer (GBO) is used in [18] to estimate the parameters of solar cells and PV modules in an efficient and precise manner. To show the GBO ability to estimate the parameters of solar cells, three popular solar cell models are used. Compared to the experimental, the suggested GBO achieves a high degree of closeness between the simulated V-P and V-I curves.

The work in [19] provided an improved chaotic JAYA algorithm for precisely and reliably classifying the parameters of various photovoltaic models, such as single-diode and

double-diode models. Furthermore, on multiple phases of the search space, the proposed method includes a self-adaptive weight to govern the trend and obtain the ideal solution while avoiding the worst result. Compared to previous algorithms in the literature, comprehensive analysis and practical results show that the proposed algorithm achieved highly competitive efficiency in terms of accuracy and dependability. In [20], a numerical approach is proposed for finding the five-parameter model of photovoltaic cells. To investigate the relationships between parameters, explicit equations are used, which are then solved by an optimization method. The suggested approach produces accurate results, and it can be used with a variety of solar cells. This paper proposed a classified perturbation mutation-based particle swarm optimization algorithm [21]. The performance of each updated personal best position is evaluated and quantified as high-quality or low-quality during each generation of the suggested algorithm. The presented technique outperformed other well-known parameter extraction methods in terms of accuracy, stability, and speed, as demonstrated by the results of the experiments. This paper proposed an improved wind-driven optimization approach for identifying the nine unknown parameters [22]. The suggested technique is a hybrid of the differential evolution algorithm mutation strategy and the wind-driven optimization algorithm covariance matrix adaption evolution strategy. The findings showed that in terms of accuracy, convergence speed, and practicality, the revised wind-driven optimization model surpassed the other models.

Based on the literature, most researchers applied their algorithms to determine the cell/module parameters without testing those parameters in emulating the behavior of a complete array. Therefore, the certainty of the identified parameters has not been validated with simulating an entire PV string or array under different environmental conditions. Further, proposing the reliable and efficient optimizer to determine the PV models parameters with high certainty for implementing its physical behaviors is a challenging task because the actual values of the model parameters are unknown, so any improvement in fitting accuracy is regarded as highly beneficial from a modeling standpoint [12]. Furthermore, the No Free Lunch theorem in [23] states that no one method can handle all optimization issues. As a result, the search for an alternate optimization technique to consistently identify the PV model parameters is ongoing.

Therefore, this paper introduced a new metaheuristic search method for parameter extraction of PV models using a modified variant of the Runge Kutta (RUN) method. RUN is, without a doubt, one of the most influential and versatile search methods used today. It has the benefit of being simple to execute and effective. However, although RUN has recently been used to tackle various real-world problems, it has a significant issue in discovering the search space efficiently with nonlinear optimization problems and exploiting the solutions. Therefore, in this work, a modified variant of RUN (MRUN) is proposed to tackle these drawbacks and handle the nonlinear optimization problem of PV modeling with high accuracy and consistency. The following lines sum up the analyses through the paper:-

- A novel variant of the RUN optimizer is proposed for identifying the 1D and 2D models parameters utilizing a set of several experimental data for PV cells and modules under numerous operating conditions of radiation and temperature.
- The proposed method results are validated via Lambert equations for the two models; 1D and 2D.
- The proposed optimizer results are compared with recent meta-heretic algorithms are implemented on the same settings and well-known PV parameters extraction methods in the literature.
- The quality of the extracted model parameters is justified in implementing the physical behavior of entire systems consisting of a set of strings (S), and series-parallel (SP) arrays PV arrays subject to multiple levels of radiation and temperature.

The results show that the proposed algorithm precisely and reliably defines the parameters of different PV models besides providing extremely competing results compared to other well-known PV parameters extraction methods statistically. Furthermore, the results divulge that the proposed modification enhanced the core abilities of the optimizer. For example, MRUN is good at searching the search space and discovering the optimum global region. Moreover, it has an excellent ability at exploiting the solutions, so even when the population has not converged to a local optimum, the algorithm can find any better answers to advance the evolution. Finally, the results of the entire S and SP systems reveal the certainty of the identifying parameters in acting the PV arrays characteristics with high efficiency.

The rest sections of this paper is given as follows. Section II presents a description of the equivalent circuits. Problem definitions are given in Section III. The details of the proposed optimizer is presented in section IV. The results and discussions are established in section V. The justification process of the proposed optimizer results id presented in section 6, finally, Conclusion and future open direction are given in Section VII.

II. PHOTOVOLTAIC EQUIVALENT CIRCUITS

In this section, the basic model of Photovoltaic (PV) equivalent circuits is introduced. In general, the most popular PV models are the single diode model (1D) and the double diode model (2D) (see Fig. 1). Each of one of these models has its own characteristics; for example, 1D is considered as the simplest equivalent circuit. Whereas 2D is more efficient than 1D since 2D simulates the physical quality of PV models at low level of irradiation conditions [24]. In this model (i.e., 2D), the first and second diode stand for the diffusion current and recombination effects, respectively. The SD consists of one diode and photo that produced shunt resistance (R_{sh}) and current. After that, the integration become in series form with a resistance (R_s). Then the output PV current (I) is

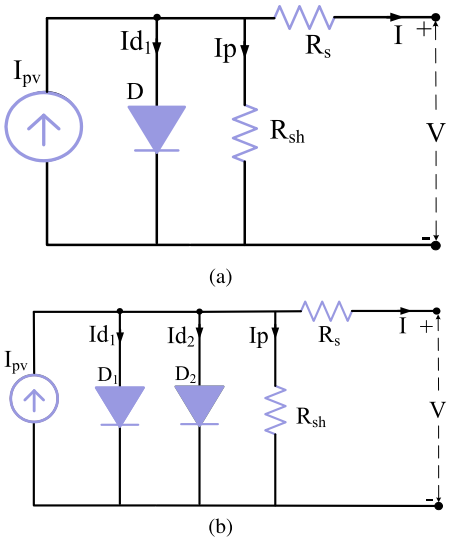

FIGURE 1. Equivalent circuits of PV: (a) Single diode model, and (b) Double diode model.

calculated based on the law of kirchhoff current as given in Eqs. (1)-(2) [7], [10], [25].

$$I = I_{ph} - I_{d1} - I_p \tag{1}$$

$$I = I_{ph} - I_{o1}\left[exp\left(\frac{V + IR_s}{a_1 V_{th}}\right) - 1\right] - \frac{V + IR_s}{R_{sh}} \tag{2}$$

In Eq. (1), a_1 is ideality factor of the diode. the I_p, I_{o1}, and I_{d1} stand for leakage shunt, saturation diode and the diode currents, respectively. Also, V_t represents the thermal voltage and it is measured at temperature (T in Kelvin) as $\frac{KT}{q}$, where $k = 1.35 \times 10^{-23} J/K$ is Boltzmann constant and $q = 1.6 \times 10^{-19} C$ denotes the electron charge.

Besides Eq. (2), there are five parameters (i.e., I_{ph}, I_{o1}, a_1, R_S, and R_{sh}) are required to be determined.

From Fig. 1(b) it can be observed that the 2D is an extension of 1D by integrating a parallel second diode with the first diode in SD. This simulates the physical influences at the P-N junction and similar to 1D, the output current of PV is computed as [7], [10], [25].:

$$I = I_{ph} - I_{o1}\left[exp\left(\frac{q(V + IR_s)}{a_1 kT}\right) - 1\right] - I_{o2}\left[exp\left(\frac{q(V + IR_s)}{a_2 kT}\right) - 1\right] - \frac{V + IR_s}{R_{sh}} \tag{3}$$

In Eq. (3), a_1 (a_2) stands for the ideality factor of first(second) diode. I_{o2} stands for the saturation current. Besides Eq. (3), there are seven parameters (i.e., I_{ph}, I_{o1}, I_{o2}, a_1, a_2, R_s, and R_{sh}) are required to be identified.

In addition, the produced photocurrent is computed based on incident radiation value (G) at T as Eq. (4a). As well as, the reverse saturation currents of $I_{o1,2}$ are computed as in Eq. (4b). While, R_{sh} depends on G and it is defined in Eq. (4d) and Eq.(4e) represents the process of computing the open circuit voltage ($V_{oc(T)}$) at temperature T [26], [27].

$$I_{ph_{(G,T)}} = I_{ph_{(s)}}\left[1 + \frac{Cf_i}{100}(T - 25)\right]\frac{G}{G_s},$$

$$G_s = 1000 W/m^2 \tag{4a}$$

$$I_{o1,2_{(T)}} = I_{o1,2_{(s)}}\left(\frac{T}{T_s}\right)^3 e^{\left(\frac{qE_g}{a_{1,2}k}\right)\left(\frac{1}{T_s} - \frac{1}{T}\right)}, \tag{4b}$$

$$T_s = 25°C \tag{4c}$$

$$R_{p_{(G)}} = R_{p_{(s)}}\left(\frac{G_s}{G}\right) \tag{4d}$$

$$V_{oc_{(T)}} = V_{oc_{(s)}}\left[1 + \frac{Cf_v}{100}(T - 25)\right] \tag{4e}$$

where $V_{oc_{(s)}}$, R_{p_s}, $I_{o1,2_s}$, and I_{ph_s} stand for the open circuit voltage, shunt resistance, reverse saturation currents, and photo current, respectively. The Cf_v ($\%/°C$) and Cf_i ($\%/°C$) denote the temperature coefficient of voltage and current, respectively. In addition, E_g stand for the band-gap energy that defined as [26], [27].:

$$E_g = E_{g_{(s)}}\left[1 - 2.6677 \times 10^{-4}(T - 25)\right] \tag{5}$$

where $E_{g_{(s)}}$ represents the band-gap energy at standard operating conditions (SOC).

III. IMPLEMENTED OBJECTIVE FUNCTION

The process of identify the parameters of the 1D and 2D is considered as a nonlinear optimization problem. The most popular objective function that used to achieve this process is the root mean square error (RMSE) that computed using the value of the estimated (I_{est}) and the measured (I_{meas}) current. To make the objective function more accurate and suitable for real-world application, the newton-raphson is used to solve the system of nonlinear equations and this can be formulated as:

$$OBJ = \sqrt{\frac{1}{M}\sum_{i=1}^{M}\left(I_{meas_i} - I_{est_i}\left(V_{meas_i}, \vec{Z}\right)\right)^2} \tag{6}$$

where Z stand for the vector that contains the set of estimated parameters. Whereas, M represents the length of the measured values. To compute the value of the estimated current ($I_{est_{t+1}}$), the extracted parameters are used with find the solution of Eqs. 2, and 3 using Newton-raphson method as formulated in Eq. ((7)):

$$I_{est_{t+1}} = I_{est_t} - \frac{(dI)}{(dI')} \tag{7}$$

In Eq. (7), dI and dI' represent the a difference function of I and its first derivative. For clarity, the definition of dI and dI' for 1D is formulated as:

$$dI = I_{ph} - I_{o1}\left[exp\left(\frac{V + I_{est_t}R_s}{a_1 V_{th}}\right) - 1\right] - \frac{V + I_{est_t}R_s}{R_{sh}} - I_{est_t}. \tag{8}$$

$$dI' = -I_{o1}\frac{R_s}{a_1 V_{th}}\left[exp\left(\frac{V + I_{est_t}R_s}{a_1 V_{th}}\right)\right] - \frac{R_s}{R_{sh}} - 1 \tag{9}$$

According to Eqs. 8-9 and substituting them in Eq. 7, then the estimated current is computed as:

$$I_{est_{t+1}} = I_{est_t} - \frac{I_{ph} - I_{o1}\left[exp\left(\frac{V+I_{est_t}R_s}{a_1 V_{th}}\right)-1\right] - \frac{V+I_{est_t}R_s}{R_{sh}} - I_{est_t}.}{-I_{o1}\frac{R_s}{a_1 V_{th}}\left[exp\left(\frac{V+I_{est_t}R_s}{a_1 V_{th}}\right)\right] - \frac{R_s}{R_{sh}} - 1} \quad (10)$$

Similar to computed $I_{est_{t+1}}$ for 1D, we can compute the $I_{est_{t+1}}$ for 2D where five iterations are enough to find the solution using Newton-raphson method.

A. VERIFYING THE RESULTS WITH LAMBERT FORM

To evaluate the performance of the identified parameters using the developed method, we used the Lambert W function (LWF) to compute the currents of 1D and 2D. The Lambert W function in mathematics is a set of functions that are the branches of the inverse relation of the β function as shown below

$$y = fexp^y \quad (11)$$

where exp^y represents the exponential function, and y is any complex number. The y of Eq.(12) can be written based on Lambert W form as follows:

$$y = f^{-1}(yexp^y) = W(\beta) \quad (12)$$

where W is the solution of the Lambert equation. By using the same concept several engineering applications can be formulated. One of those applications is solving the PV characteristic equations [28]–[30].

In general, the LWF of 1D PV model (Eq. (2)) is defined as:

$$I_{Lambert} = \frac{R_{sh}\left(I_g + I_{o1} - V\right)}{R_s + R_{sh}} - \frac{a_1 V_t}{R_s} W(\delta), \quad (13a)$$

where (13b)

$$\delta = \frac{I_{o1}R_{sh}R_s}{a_1 V_t (R_s + R_{sh})} \times exp\left(\frac{R_{sh}\left(R_s I_g + R_s I_{o1} + V\right)}{a_1 V_t\left(R_s + R_{sh}\right)}\right), \quad (13c)$$

In addition, the LWF of 2D (Eq. (2)) is defined as:

$$I_{Lambert} = \frac{R_{sh}(I_{oh} + I_{o1} + I_{o2} - V)}{R_s + R_{sh}} - r\frac{a_1 V_t}{R_s} W(\delta_1) - (1-r)\frac{a_2 V_t}{R_s} W(\delta_2) \quad (14)$$

where

$$r = \frac{I_{o1}\left[exp\left(\frac{V+IR_s}{a_1 V_t}\right)-1\right]}{I_{o1}\left[exp\left(\frac{V+IR_s}{a_1 V_t}\right)-1\right] - I_{o2}\left[exp\left(\frac{V+IR_s}{a_2 V_t}\right)-1\right]} \quad (15a)$$

$$\delta_1 = \frac{I_{o1}R_s R_{sh}}{r a_1 V_t (R_s + R_{sh})} exp\left(\frac{R_{sh}\left(R_s I_g + R_s I_{o1}/r + V\right)}{a_1 V_t\left(R_s + R_{sh}\right)}\right) \quad (15b)$$

$$\delta_2 = \frac{I_{o2}R_s R_{sh}}{(1-r) a_2 V_t (R_s + R_{sh})} \times exp\left(\frac{R_{sh}\left(R_s I_g + R_s I_{o2}/(1-r) + V\right)}{a_2 V_t\left(R_s + R_{sh}\right)}\right), \quad (15c)$$

where $I_{Lambert}$ denotes the output current obtained using LWF.

So, the RMSE has been recomputed for I_{est} using LWF according to the estimated parameters and I_{meas}. In case there is large difference ($Diff_{RMSE}$) between the RMSE (as in Eq.6) and RMSE based on LWF (i.e., $RMSE_{Lambert}$), so the process of estimated parameters is inefficient [28]–[30]. The mathematical form of $RMSE_{Lambert}$ is computed as below:

$$RMSE_{Lambert} = \sqrt{\frac{1}{M}\sum_{i=1}^{M}\left(I_{meas_i} - I_{Lambert_i}\right)^2} \quad (16)$$

IV. MODIFIED ALGORITHM BASED ON RUNGE KUTTA METHOD

In this section, the proposed enhanced Algorithm Based on Runge Kutta Method (MRUN) is proposed to modify the classical RUn optimizer performance. The details of the proposed are described below in the following subsections.

A. OVERVIEW OF THE BASIC ALGORITHM BASED ON RUNGE KUTTA (RUN) METHOD

The RUN optimization algorithm is inspired by the Runge Kutta method (RKM) [31] that was applied to find the solution for the ordinary differential equations. In general, RKM generates a high-precision numerical value based on the functions only and doesn't require any gradient information (Zheng & Zhang, 2017). Therefore, the RUN optimization algorithm depends on computing the slope in RKM, that used as a searching strategy to emulate the exploration ability in swarm-based optimization. The mathematical formulation of the RUN algorithm contains a set of stages that are discussed as follows:

- Initialization stage: In this stage, the initial solutions of N agents are constructed based on the boundaries of the search landscape [LB, UB]. This step is conducted using the following formula:

$$Z_{i,j} = LB_j + r_1 \times (UB_j - LB_j), \quad i = 1, 2, \ldots, N, \quad j = 1, 2, \ldots, D \quad (17)$$

  where D represents the dimension of the given problem. The LB_j and UB_j are the lower and upper boundaries of j^{th} variable in the solution set $Z_{i,j}$; i = 1,2, . . . , N, the symbol N refers to the total number of search agents.
- Updating solutions stage: The RUN algorithm uses a search mechanism (SM) based on the Runge Kutta method to update the position of current solution at each

iteration, which is defined as:

$$Z_i = \begin{cases} Z_{CF} + S_{FM} + \mu \times randn \times Z_{mc} \\ \qquad\qquad if\ rand \le 0.5 \\ Z_{mF} + S_{FM} + \mu \times randn \times Z_{ra} \\ \qquad\qquad otherwise \end{cases} \quad (18)$$

where $Z_{CF} = (Z_c + r \times SF \times g \times Z_c)$ and $S_{FM} = SF \times SM$. $Z_{mF} = (Z_m + r \times SF \times g \times Z_m)$. $Z_{ra} = (Z_{r1} - Z_{r2})$ and $Z_{mc} = (Z_m - Z_c)$. $r \in [-1, 1]$ is an integer number used to change the search process direction. The symbols of $g \in [0, 2]$ and $\mu \in [0, 1]$ are random numbers. The SF represents adaptive factor that defined as:

$$SF = 2.(0.5 - rand) \times f;$$
$$where$$
$$f = a \times exp\left(-b \times rand \times \left(\frac{t}{Maxt}\right)\right) \quad (19)$$

where $Maxt$ denotes the total number of iterations. Tthe Z_c and Z_m given in Eq. (18) are defined as below:

$$Z_c = \varphi \times Z_i + (1 - \varphi) \times Z_{r1} \quad (20)$$
$$Z_m = \varphi \times Z_b + (1 - \varphi) \times Z_{pb} \quad (21)$$

In Eq. (21), the $\varphi \in [0, 1]$ denotes a random number. The symbols of Z_b and Z_{pb} stand for the best-so-far agent and the best one at each iteration, respectively.
For the SM parameter that defined in Eq. (18) is updated using the following formula:

$$SM = \frac{1}{6}(Z_{RK})\,\Delta Z;$$

where

$$\begin{aligned} Z_{RK} &= k_1 + 2 \times k_2 + 2 \times k_3 + k_4 \\ k_1 &= \frac{1}{2\Delta Z}(rand \times Z_{\mathrm{w}} - u \times Z_{\mathrm{b}}), \\ k_2 &= \frac{1}{2\Delta Z}(rand.(Z_{\mathrm{w}} + rand_1.k_1.\Delta Z) - UZ \\ k_3 &= \frac{1}{2\Delta Z}(rand.(Z_{\mathrm{w}} + rand_1.\left(\frac{1}{2}k_2\right).\Delta Z) - UZ_b \\ k_4 &= \frac{1}{2\Delta Z}(rand.(Z_{\mathrm{w}} + rand_1.k_3.\Delta Z) - UZ_{b2} \\ u &= round(1 + rand) \times (1 - rand) \\ UZ &= (u.Z_{\mathrm{b}} + rand_2.k_1.\Delta Z)) \\ UZ_b &= (u.Z_{\mathrm{b}} + rand_2.\left(\frac{1}{2}k_2\right).\Delta Z)) \\ UZ_{b2} &= (u.Z_{\mathrm{b}} + rand_2.k_3.\Delta Z)) \end{aligned} \quad (22)$$

where $rand_1$ and $rand_2$ stand for random numbers. The value of ΔZ is computed as:

$$\Delta Z = 2 \times rand \times |Stp|;$$

where

$$Stp = rand \times \left(\left(Z_b - rand \times Z_{avg}\right) + \gamma\right)$$
$$\gamma = rand \times (Z_n - rand \times (u - l)) \times \exp(-4 \times \frac{t}{Maxt}) \quad (23)$$

where the value of Z_b and Z_w are updated as:

if $f\,(Z_i) < f\,(Z_{pb})$
$\quad Z_b = Z_i$
$\quad Z_w = Z_{pb}$
else
$\quad Z_b = Z_{pb}$
$\quad Z_w = Z_i$
end

- Enhanced solution quality stage: In this stage, the quality of solutions is enhanced using different operators to improve the convergence rate with skipping the local optima. This process is defined as:

$$Z_{new2} = \begin{cases} Z_{new1} + r \times \omega \times |\left(Z_{new1} - Z_{avg}\right) + randn| \\ \qquad\qquad if\ \omega < 1 \\ (Z_{new1} - Z_{avg}) + r \times \omega \times Z_{na} \\ \qquad\qquad otherwise \end{cases} \quad (24)$$

$$\begin{aligned} Z_{na} &= |\left(u \times Z_{new1} - Z_{avg}\right) + randn| \\ \omega &= rand(0,\ 2).exp\left(-c\left(\frac{t}{Maxt}\right)\right), \\ c &= 5 \times rand \\ Z_{avg} &= \frac{Z_{r1} + Z_{r2} + Z_{r3}}{3} \\ Z_{new1} &= \beta \times Z_{avg} + (1 - \beta) \times Z_b \end{aligned} \quad (25)$$

In Eq. (25), $\beta \in [0, 1]$ represents random number and $r \in \{1, 0, -1\}$ is an integer number.
Following [31], in case the fitness value of Z_{new2} not better than the fitness value of Z_i then there is another chance to modify the the value of Z_i. The solutions can be updated using the following formula:

$$\begin{aligned} Z_{new3} &= (Z_{new2} - r_1 \times Z_{new2}) + SF \times D_Z, \\ D_Z &= (r_2 \times Z_{RK} + (v \times Z_b - Z_{new2})) \end{aligned} \quad (26)$$

where $v = 2 \times r_3$ is a random number stands for the interval of $2 \times [0\ 1]$. r_1, r_2 and r_3 are random values.

The pseudo-code of the classical RUN is exhibited in algorithm 1 to summarize the main steps of the algorithm structure.

B. STEPS OF THE PROPOSED MODIFIED RUN (MRUN)

As described in the previous section of classical RUN, the main two stages are updating the solutions and enhancing them. In updating the solution stage, the transition process between the exploration and exploitation stage based on a random process where if rand ≤ 0.5, the exploration phase

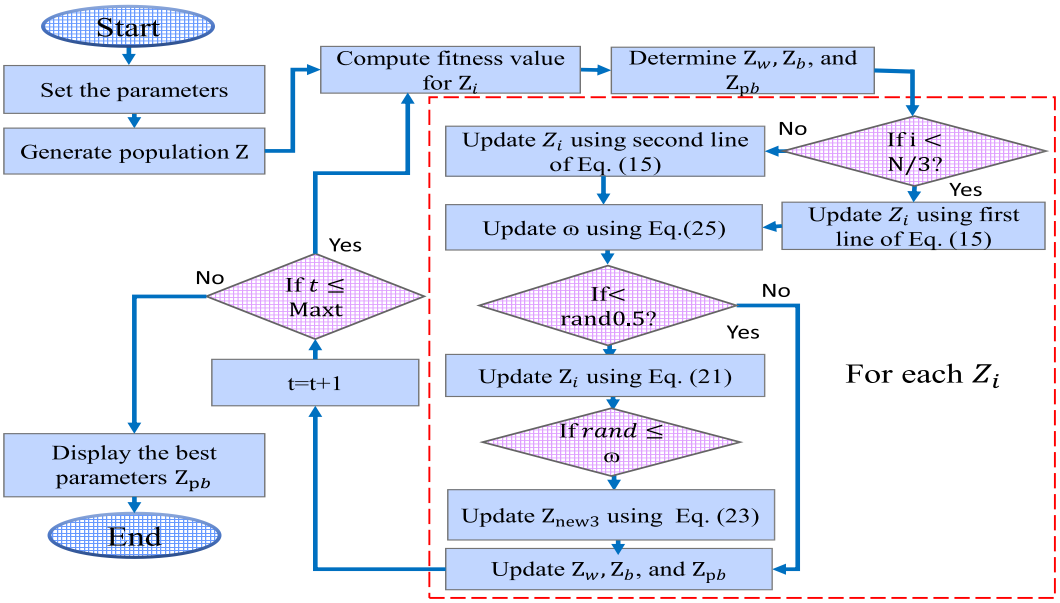

FIGURE 2. Flowchart of MRUN optimizer.

TABLE 1. Electrical specifications of the PV solar cell/module.

Parameters	RTC France cell	KC200GT PV panel	NU-(Q250W2) PV panel	Pythagoras Solar Large PVGU Window
P_{max} (W)	0.3101	200.143	250	271
V_{mp} (V)	0.459	26.3	30.3	48.4
I_{mp} (A)	0.6755	7.61	8.26	5.6
V_{oc} (V)	0.536	32.9	37.6	58.2
I_{sc} (A)	0.7605	8.21	8.9	6
N_s	1	54	60	90
NOCT ($^{\circ}C$)	45	45	47.5	45
Cf_i (% $/^{\circ}C$)	0.036	0.06	0.074	-0.14
Cf_v (% $/^{\circ}C$)	-0.370	-0.329	-0.35	-0.32199

The Cf_v and Cf_i denote the voltage and current temperature coefficients,respectively

is performed else the exploitation phase is implemented. Such of this approach may be cause inconsistency in the attained solutions by the RUN. For modifying this process, in MRUN, the transition process between the exploration and exploitation phases is divide in the search agents where in the first third of the search agents group the exploration is performed and for the rest of the agents the exploitation is executed as reported in Algorithm 2. Furthermore, in the MRUN, the main controller variable in the enhanced solution stage ω is modified via using pareto heavy-tied distribution of Eq.27 rather than uniform distribution rand(0,2) to enhance the new solutions Z_{new2}. Pareto distribution (PF): a random variable has been shown to follow Pareto distribution if it has the following tail function PF:

$$PF(x) = \begin{cases} 1 - \left(\frac{b}{x}\right)^a, & x \geq b \\ 0, & x < b \end{cases} \tag{27}$$

where a, and b are the scale and shape parameters and have values of 0.0001 and 2, respectively. the x is random vector with dimension (1,D). Then the updated ω based on PF is written as follows:

$$\omega = PF.exp\left(-c\left(\frac{t}{Maxt}\right)\right), \quad c = 5 \times rand \tag{28}$$

The Fig.2 depicts the flowchart of the proposed MRUN. The algorithm starts with set of random solution while these solutions are modified using Algorithm 2 in the updated solution stage and employing pareto front in the phase of enhancing the solutions of Eqs. 24, 28, 26.

V. SIMULATIONS AND DISCUSSIONS

The proposed ERIN is assessed throughout several sets of experimental series. Firstly, the proposed optimizer is applied to identify the parameters of 1D and 2D models using RTC France datasets. Then, in the second series of experiments, the parameters of 2D models of three modules including Kyocera Solar KC200GT PV module, Sharp NU-(Q250W2) panel and Pythagoras Solar Large PVGU

Algorithm 1 Pseudo-Code of the RUN

Initialize the seach agents N, maximum number of iterations $Maxt$. define the search space boundaries (LB, UB).
Using Eq. (17) to generate the initial population Z.
while (t < Maxt) **do**
  Compute fitness for each solution with determine the best (Z_b), worst Z_w and Z_{pb} solutions.
  for ($i = 1$ to N) **do**
    for ($j = 1$ to D) **do**
      Using Eq. (18) to update Z_i.
      if $rand < 0.5$ **then**
        Using Eq. (24) to obtain Z_{new2}
        if $F(Z_i) < F(Z_{new2})$ **then**
          if $rand < w$ **then**
            Using Eq. (26) to obtain Z_{new3}.
          end if
        end if
      end if
    end for
  end for
  t=t+1
end while
Return the best solution (Z_b).

Algorithm 2 Pseudo-Code of Enhancing the Updated Solution Stage of the Classical RUN

for ($i = 1$ to N) **do**
  if i< $N/3$ **then**
    Use the following formula
    $Z_i = (Z_c + r \times SF_i \times g \times Z_c) + SF_i \times SM + \mu \times (Z_m - Z_c)$ (exploration)
  else
    Use the following formula
    $Z_i = (Z_m + r \times SF_i \times g \times Z_m) + SF_i \times SM + \mu \times (Z_{r1} - Z_{r2})$ (exploitation)
  end if
end for

Window under different operating conditions of temperature and irradiation. The manufacture properties of the realized panels at SOC are reported in Table 1. The MRUN technique results are compared with set of optimization techniques including aquila optimizer (AO) [32], electric fish optimizer (EFO) [33], barnacles mating optimizer (BMO) [34], capuchin search algorithm (CapSA) [35], and red fox optimization algorithm (RFSO) [36] to investigate the proposed performance. The setting values of the population size, number of iterations and number of independent runs are 50, 500 and 25, respectively. These values are applied for all the implemented algorithms for achieving unbiased comparison. The upper (B_{max}) and lower (B_{min}) boundaries for the realized models unknown parameters are tabulated in Table 2.

TABLE 2. The lower and upper limits of the search space of 1D and 2D variables.

PV cell (1D/2D) [7]			PV modules (2D)		
Parameters	B_{min}	B_{max}	Parameters	B_{min}	B_{max}
$R_s(\Omega)$	0	0.5	$R_s(\Omega)$	0.001	2
$R_p(\Omega)$	0	100	$R_p(\Omega)$	0.001	500
$I_{pv}(A)$	0	2	$I_{pv}(A)$	0	10
$I_{o1}(\mu A)$	0	2	$I_{o1}(\mu A)$	10^{-6}	1
$I_{o2}(\mu A)$	0	2	$I_{o2}(\mu A)$	10^{-6}	1
a_1	1	2	a_1	1	5
a_2	1	2	a_2	1	5

where LB is lower bounds and UB is the upper boundaries

A. MODELING OF PV SOLAR CELL

In this section a set of 26 (V-I) measured pairs for a commercial RTC France silicon solar cell at $1000W/m^2$ and $33°C$ is used while evaluating the performance of the proposed optimizer. The identified parameters of 1D and 2D models by MRUN, other peers and set of recent literature are reported in Table 3 with the established fitness function value (RMSE) as a primary metric for the accuracy of the results. Moreover, the accuracy of the estimated parameters is evaluated though implementing Lambert forms for 1D and 2D models of section III-A to compute the $RMSE_{lambert}$ then calculating the deviation ($Diff_{RMSE}$) between the $RMSE_{lambert}$ and the attained RMSE of Eq. (6), the large deviation refers to an inefficient identified parameters. Furthermore, the absolute error at MPP (AE_{MPP}) is reported in the Table 3 for providing an extensive analysis.

From the results given in Table 3, it can be noticed that RMSE and $Diff_{RMSE}$ by MRUN is smaller than other implemented techniques (RUN, AO, EFO, BMO, CaSA, RFSO) in the two test cases (i.e., 1D and 2D). This indicates the high performance of the developed MRUN approach and affirm its superiority over the other approaches. The AE_{MPP} values by the MRUN show its reliability in modeling the PV solar cell with high accuracy.

For further analysis of the performance of MRUN, different statistical measures are used. These measures are the best, worst, average, median, variance, and standard deviation (StD). The Wilcoxon signed-rank test is also applied to if the difference between the MRUN and other methods is significant or not, and this is evaluated at a significant level of 0.05. From these tabulated results, it can be observed that MRUN allocates the first rank in terms of best, worst, average, and median. In addition, its stability is better than other methods. The traditional RUN can provide better results than the different algorithms; however, BMO is competitive. Moreover, the p-value obtained using the Wilcoxon signed-rank test indicates a significant difference between MRUN and other methods.

For affirm the certainty of the identified parameters, Fig. 3 and Fig. 4 are reported to depict the current- voltage (V-I) characteristic, Power-voltage (V-P) characteristic, absolute error curve between measured and estimated datasets, Mean convergence curve and RMSE throughout 25 independent times using 1D and 2D model of RTC France solar cell,

TABLE 3. The identified parameters by the proposed technique versus peers under different radiations and temperatures for 1D and 2D of RTC France cell.

		Parameters										
Mod	Alg	a_1	a_2	$R_s(\Omega)$	$R_p(\Omega)$	$I_{o1}(A)$	$I_{o2}(A)$	$I_{ph}(A)$	RMSE	$RMSE_{lambert}$	$Diff_{RMSE}$	AE_{MPP}
1D	MRUN	1.4769		0.036556	52.8443	$3.101e-07$		0.76079	0.00077301	0.00077301	$4.2501e-17$	$4.4135e-05$
	RUN	1.48		0.036416	53.3271	$3.1973e-07$		0.76079	0.00077438	0.00077438	$1.5417e-16$	$8.3735e-05$
	AO	1.4935		0.049813	68.6271	$3.2013e-07$		0.7525	0.025838	0.025838	$2.3245e-16$	0.0062191
	EFO	1.474		0.036776	51.7497	$3.0103e-07$		0.76085	0.00079124	0.00079124	$-5.2584e-17$	$5.8611e-05$
	BMO	1.4827		0.036306	54.4458	$3.2868e-07$		0.76074	0.00077817	0.00077817	$1.3151e-16$	0.0001101
	CapSA	1.4961		0.036049	68.1427	$3.7559e-07$		0.76043	0.00096009	0.00096009	$1.8215e-17$	$9.1438e-05$
	RFSO	1.6045		0.030998	97.4083	$1e-06$		0.76072	0.0021177	0.0021177	$6.2016e-17$	0.0015235
2D	MRUN	1.9013	1.4151	0.037204	56.2764	$9.9935e-07$	$1.4361e-07$	0.76075	0.00074653	0.00076138	$1.4847e-05$	0.00012692
	RUN	1.6103	1.2749	0.037655	58.0506	$6.043e-07$	$1.2832e-08$	0.7607	0.00075861	0.00081235	$5.374e-05$	0.00010591
	AO	1.7564	1.5797	0.037464	63.4863	$7.2605e-07$	$6.8876e-07$	0.7659	0.020189	0.020186	$-2.9365e-06$	0.005578
	EFO	1.4616	1.2118	0.037469	49.4015	$2.6571e-07$	$1e-12$	0.76099	0.00086828	0.0008683	$2.2749e-08$	$3.8385e-05$
	BMO	1.4724	2	0.036748	51.7853	$2.9651e-07$	$1e-12$	0.76082	0.00077644	0.00077644	$1.7815e-12$	$9.4841e-06$
	CapSA	1.9979	1.5283	0.034498	74.7048	$1e-12$	$5.0977e-07$	0.76004	0.0011631	0.0011631	$-2.6443e-11$	0.00070459
	RFSO	1.8335	1.6046	0.030574	79.9941	$1e-12$	$1e-06$	0.7607	0.0021895	0.0021895	$-3.88e-11$	0.0017306

TABLE 4. Statistical metrics for the obtained results by MRUN, RUN and other concurrent during handling the 1D and 2D models of the RTC.France cell.

		Statically metrics						Wilcoxon signed-rank test MRUN vs others			
Cond	Alg	Best	Worst	Average	Median	Variance	Std	R_+	R_-	p_{value}	h_o
1D	MRUN	0.00077301	0.00079618	0.00077605	0.00077478	2.4304e-11	4.9299e-06	-	-	-	-
	RUN	0.00077438	0.0020642	0.0011837	0.0010905	1.2815e-07	0.00035798	322	3	1.7735e-05	1
	AO	0.025838	0.13818	0.072948	0.069389	0.00084789	0.029118	325	0	1.229e-05	1
	EFO	0.00079124	0.0014354	0.00099223	0.00097659	2.5026e-08	0.0001582	325	0	1.229e-05	1
	BMO	0.00077817	0.002171	0.0013234	0.0012874	1.852e-07	0.00043035	325	0	1.229e-05	1
	CapSA	0.00096009	0.0026484	0.0018895	0.0020833	1.4902e-07	0.00038603	325	0	1.229e-05	1
	RFSO	0.0021177	0.013458	0.0050678	0.0034187	1.4695e-05	0.0038334	325	0	1.229e-05	1
2D	MRUN	0.00074653	0.0010947	0.00078348	0.00076615	5.3151e-09	7.2905e-05	-	-	-	-
	RUN	0.00075861	0.0022083	0.0011295	0.00095536	1.6889e-07	0.00041096	302	23	0.00017437	1
	AO	0.020189	0.12443	0.073902	0.079246	0.00078095	0.027945	325	0	1.229e-05	1
	EFO	0.00086828	0.0014667	0.0010438	0.001023	2.1998e-08	0.00014832	325	0	1.229e-05	1
	BMO	0.00077644	0.011716	0.0025072	0.0020833	4.075e-06	0.0020187	321	4	2.0013e-05	1
	CapSA	0.0011631	0.0027489	0.0022754	0.0022568	1.5088e-07	0.00038844	325	0	1.229e-05	1
	RFSO	0.0021895	0.013931	0.0051489	0.0033068	1.497e-05	0.003869	325	0	1.229e-05	1

where $h_o = 1$ refers to existence of a significant difference between the MRUN and the other optimizers.

respectively. From these graphs it can be reached to the following observations; the identified parameters by MRUN provides a closely matching between the measured and estimated that sets. This observation is confirmed from the absolute error curves of Figs.3(c)-4(c) for 1D and 2D models, respectively. The mean convergence rate of MRUN of Figs. 3(d)-4(d) converges to the highest quality solutions compared to the other techniques. In addition, the boxplots of RMSE of Figs.3(e)-4(e) indicate the high stability of MRUN in 1D and 2D models. Followed by EFO and CapSA, however, AO is the worst algorithm in both models.

To justify the performance of MRUN, it is compared with well-known PV parameters estimation methods in which their results are collected from literature. These methods including cuckoo search (CS) [37], multiple learning backtracking search algorithm (MLBSA) [38], modified PSO (MPSO) [39], improved cuckoo search algorithm (CSA) and (ICSA) [40], improved whale optimization algorithm variants (CWOA) and (PSO-WOA) [12], improved shuffled complex evolution algorithm (ISCE) [41], fractional chaotic ensemble particle swarm optimizer (EPSO) [42], chaos PSO (CPSO) [43], chaotic heterogeneous comprehensive learning PSO (HCLPSO) [44], self-adaptive teaching-learning-based optimization (STLBO) [45], hybrid firefly and pattern search algorithms (HFAPS) [46], time varying acceleration coefficients particle swarm optimisation (TVACPSO) [47], genetic algorithm (GA) [48], performance-guidedJAYA (PGJAYA) [49], chaotic whale optimizer (CWOA) [50], gravitational search algorithm (GSA) [51], and parallel PSO (PPSO) [52].

The results of Table 6 reveal that the developed MRUN provides the most powerful results in comparison to most of the recent state-of-the-art techniques. Meanwhile, the MRUN has the same RMSE similar to TVACPSO and CPSO when applied to determine the parameters of the 1D model. For the 2D, the MRUN statistical metrics values prove the algorithm superiority in providing the most accurate results with comparable execution time.

B. MODELING OF PV SOLAR COMMERCIAL MODULES

Within this section, the developed method has been applied to determine the parameters of 2D model of KC200GT solar panel, Sharp NU-(Q250W2) panel, and Pythagoras Solar Large PVGU Window under three different operating conditions for each module.

Table 9 shows the results of the developed MRUN and other methods using KC200GT, Sharp NU-(Q250W2), and Pythagoras Large PVGU Window PV module for 2D model. It can be noticed from the reported data that the high efficiency of the MRUN algorithm at the three different cases (i.e., at different temperatures). Since the $Diff_{RMSE}$ of MRUN is zeros among all the tested cases. However, it has been observed that the performance of other models are decreased at $1000W/m^2$ 45 $^\circ C$ in the three PV module.

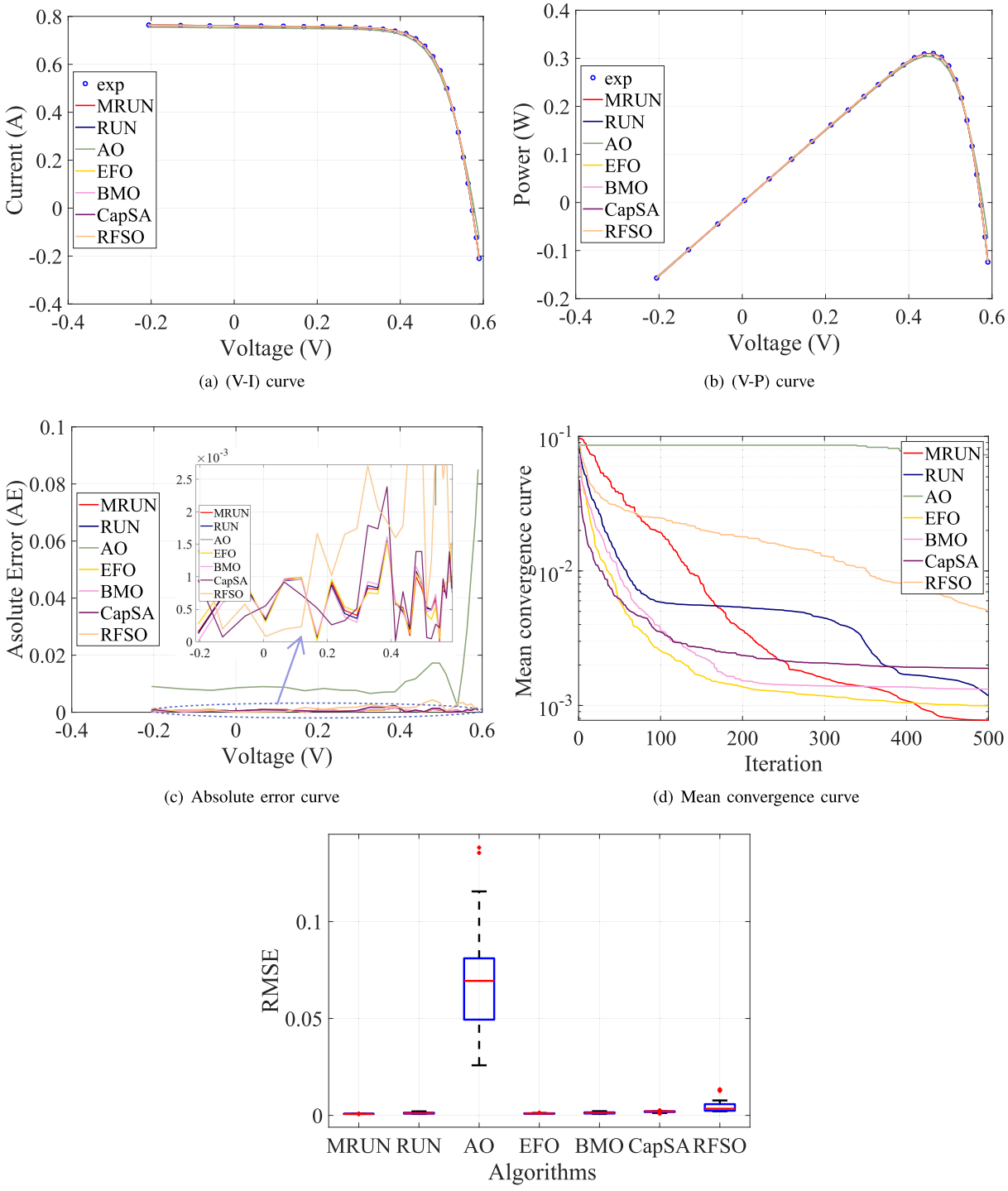

(a) (V-I) curve

(b) (V-P) curve

(c) Absolute error curve

(d) Mean convergence curve

(e) RMSE values

FIGURE 3. The implemented optimizers responses in case of 1D model of RTC france solar cell throughout 25 separate times.

In some cases, the quality of other compared algorithms at $1000W/m^2$ $60\,^{\circ}C$ is better than at $1000W/m^2$ $45\,^{\circ}C$ and $1000W/m^2$ $25\,^{\circ}C$.

Furthermore, the V-I, V-P characteristics, and AE curves are plotted in Figs. 5- 6, and 7 respectively. The figures show the high matching between the measured and estimated datasets of the three studied models, manning the identified parameters high accuracy. The mean convergence curves of MRUN is better than the competitive algorithms (i.e., RUN, AO, EFO, BMO, CapSA, and RFSO).

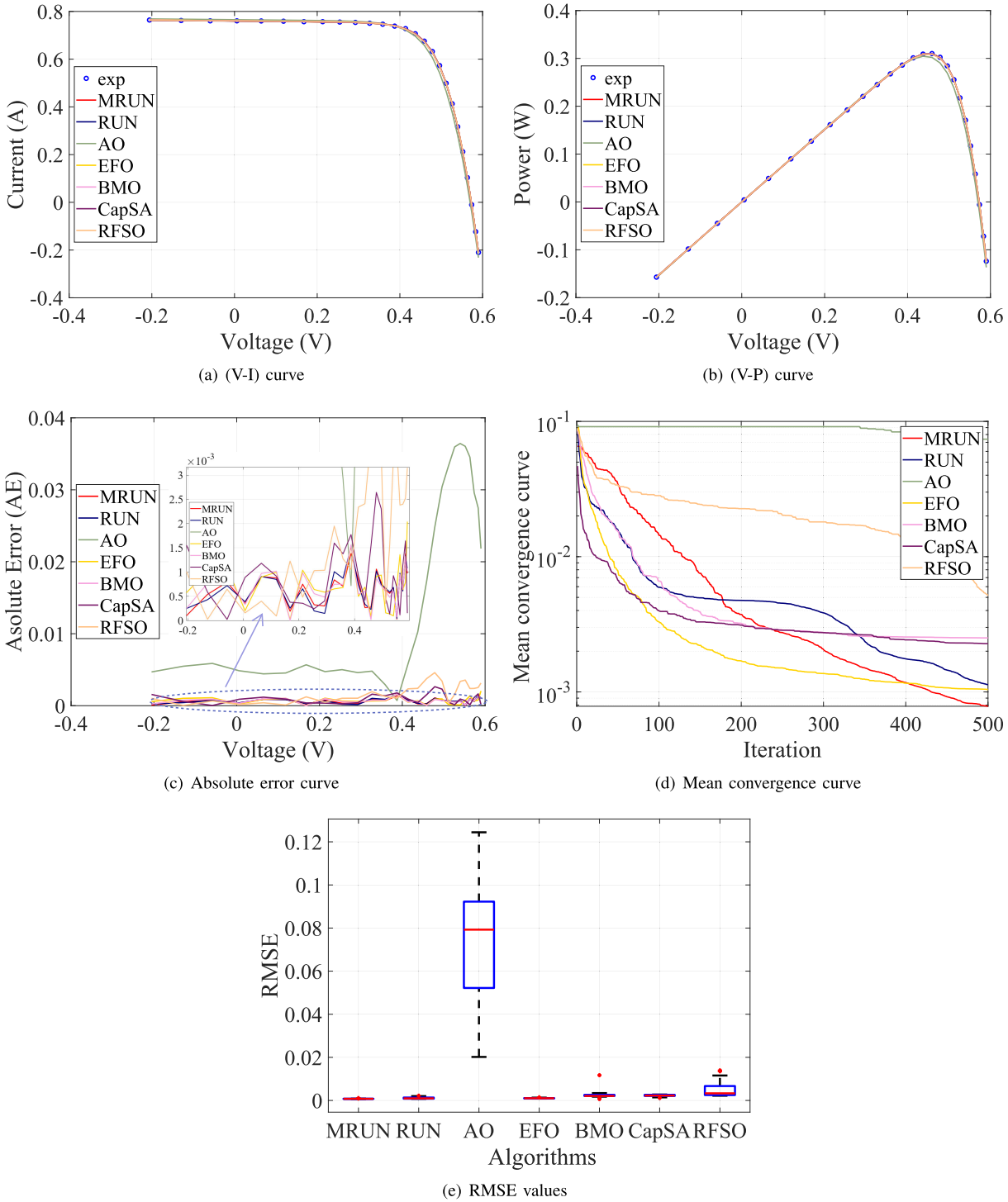

(a) (V-I) curve

(b) (V-P) curve

(c) Absolute error curve

(d) Mean convergence curve

(e) RMSE values

FIGURE 4. **The implemented optimizers responses in case of 2D model of RTC france solar cell throughout 25 separate runs.**

For the statistical evaluation part, the difference between the developed MRUN and RUN is significant in all cases, as noticed from the P-value obtained by Wilcoxon signed-rank test. In addition, the MRUN can get results better than RUN in terms of Best, Worst, Average, Median. Also, the developed MRUN is more stable than traditional RUN among the tested cases.

The accuracy of the extracted parameters is tested for further assessment while emulating the PV modules characterises under different operating irradiation, and temperature

TABLE 5. Statistical metrics employed to evaluate the performance of the proposed MRUN.

Metric	Formula	Metric	Formula
RMSE	$\sqrt{\frac{1}{M}\sum_{i=1}^{M}(I_m - I_e)^2}$	Weighted RMSE (ξ)	$\frac{RMSE}{I_{sc}}$
Summation Absolute Error (SAE)	$\sum_1^M \lvert I_m - I_e \rvert$	Mean Absolute Error (MAE)	$\sum_1^M \frac{\lvert I_m - I_e \rvert}{M}$
Sum Squared Error (SSE)	$\sum_1^M (I_m - I_e)^2$	Mean Bias Error (MBE)	$\sum_1^M \frac{I_m - I_e}{M}$

where I_m, I_e are the measured and estimated currents.

TABLE 6. Statistical analysis by MRUN versus recent state-of-the-art algorithms in case of RTC France solar cell and CPU time (sec).

		Statistical Analysis						
	Models/Techs	RMSE ± STD	ξ	SAE	MAE	SSE	MBE	CPU time (sec)
1D	**MRUN**	$7.7301e-04 \pm 4.9299e-06$	$1.0167e-03$	$1.7634e-02$	$6.7824e-04$	$1.5536e-05$	$-1.8244e-07$	44.0057
	EPSO	$8.0621e-04 \pm 4.3109e-04$	$1.0604e-03$	$1.8787e-02$	$7.2259e-04$	$1.6900e-05$	$-1.0023e-05$	13.6707
	PGJAYA [49]	$9.8602e-04 \pm 1.4485e-09$	$1.2966e-03$	–	$1.2969e-03$	–	–	41
	CWOA [12]	$9.98678e-04 \pm 6.33831e-03$	$1.3132e-03$	–	–	–	–	–
	PSO-WOA [12]	$1.07101e-03 \pm 1.17001e-03$	$1.4083e-03$	–	–	–	–	–
	SATLBO [45]	$9.86022e-04 \pm 2.3002e-06$	$1.2965e-03$	–	–	–	–	–
	HFAPS [46]	$9.8602e-04 \pm -$	$1.0164e-03$	–	–	–	–	–
	MLBSA [38]	$9.8602e-04 \pm 9.1461e-12$	$1.2965e-03$	–	$7.5e-03$	–	–	–
	TVACPSO [47]	$7.7301e-04 \pm 5.5805e-10$	$1.2965e-03$	–	–	–	–	44
	CPSO [47]	$7.7301e-04 \pm 2.8344e-5$	-	–	–	–	–	–
	GSA [51]	$4.1020e-03 \pm 2.7197e-03$	-	–	–	–	–	–
	CSA [40]	$9.86023e-04 \pm 8.570571e-06$	-	–	–	–	–	–
	ICSA [40]	$9.8602e-04 \pm 2.987589e-12$	-	–	–	–	–	–
	GA [48]	$19.08e-03 \pm -$	-	–	–	–	–	–
	CS [37]	$1.000e-03 \pm -$	-	–	–	–	–	–
			-	–	$7.00e-4$	–	–	–
	HCLPSO [44]	$7.89580e-04 \pm 3.0090e-04$	$1.03851e-03$	$1.83898e-02$	$7.07300e-04$	$1.62093e-05$	$6.48591e-07$	204.5567
	ISCE [41]	$9.86022e-04 \pm -$	$1.29688e-03$	$1.77041e-02$	$6.80926e-04$	-	-	
	CWOA [50]	$9.8600e-04 \pm -$	$1.29686e-03$	$2.15280e-02$	$8.2800e-04$	-	$7.2800e-08$	
	BMO [50]	$9.8608e-4 \pm -$	$1.29696e-03$	$2.20480e-02$	$8.4800e-04$	-	$1.1302e-06$	
	STLBO [50]	$9.8602e-04 \pm -$	$1.29688e-03$	$2.15540e-02$	$8.2900e-04$	-	$4.0948e-7$	
	EHA-NMS [53]	$9.8602e-04 \pm -$	$1.2965e-03$	$1.7704e-02$	$6.80923e-04$	-	-	
	NM-MPSO [54]	$9.8602e-04 \pm -$	$1.2965e-03$	$1.19548e-01$	$4.5980e-03$	-	-	
	PPSO [52]	-	-	$1.77798e-02$	$6.8384e-04$	-	-	
	FPA [55]	$7.7301e-04 \pm -$	$1.01672e-03$	$1.5971e-02$	$6.14269e-04$	$5.181638e-06$	-	
	MPSO [39]	$9.8602e-04 \pm -$	$1.2965e-03$	-	-	-	-	
	CPSO [43]	$2.6500e-03 \pm -$	$3.48547e-03$	$1.6800e-03$	$1.6800e-03$	-	$6.100e-05$	
2D	**MRUN**	$7.4653e-04 \pm 7.2905e-05$	$9.8189e-04$	$1.7137e-02$	$6.5913e-04$	$1.449e-05$	$-2.9284e-05$	2.498
	EPSO [42]	$7.6312e-04 \pm 1.5424e-04$	$1.0037e-03$	$1.7439e-02$	$6.7075e-04$	$1.5141e-05$	$-6.5272e-06$	15.4857
	PGJAYA [49]	$9.8263e-04 \pm 2.5375e-06$	$1.4859e-03$	–	–	–	–	–
	CWOA [12]	$1.130041e-03 \pm 2.153407e-03$	$2.1959e-03$	–	–	–	–	–
	PSO-WOA [12]	$1.669996e-03 \pm 9.551144e-04$	$1.2923e-03$	–	–	–	–	–
	SATLBO [45]	$9.828037e-04 \pm 1.951533e-05$	$9.7620e-04$	–	–	–	–	–
	HFAPS [46]	$9.8248e-04 \pm -$	$1.2919e-03$	–	–	–	–	–
	MLBSA [38]	$9.8249e-04 \pm 1.3482e-06$	$1.2919e-03$	–	$7.1e-03$	–	–	39
	GA [51]	$5.91958e-03 \pm 1.818e-03$	-	–	–	–	–	–
	CSA [40]	$9.8292e-04 \pm 4.1755e-06$	-	-	-	-	-	-
	ICSA [40]	$9.8249e-04 \pm 2.8197e-07$	-	-	-	-	-	-
			-	-	-	-	-	-
			-	-	-	-	-	-
	HCLPSO [44]	$7.6680e-04 \pm 1.8624e-04$	$1.0086e-03$	$1.7399e-02$	$6.6919e-04$	$1.5288e-05$	$-1.3767e-05$	265.3884
	ISCE [41]	$9.8248e-04$	$1.2922e-03$	$1.7319e-02$	–	–	–	
	CWOA [50]	$9.8279e-04$	$1.2926e-03$	$2.1294e-02$	$8.1900e-04$	-	$1.23263e-07$	
	BMO [50]	$9.8262e-04 \pm -$	$1.2924e-03$	$2.1554e-02$	$8.2900e-04$	-	$5.8807e-07$	
	STLBO [50]	$9.8248e-04 \pm -$	$1.2922e-03$	$2.3348e-02$	$8.9800e-04$	-	$1.3684e-07$	
	EHA-NMS [53]	$9.8248e-04 \pm -$	$1.2923e-03$	$1.7319e-02$	$6.6612e-04$	-	-	
	NM-MPSO [54]	$9.8250e-04 \pm -$	$1.2919e-03$	$11.6610e-02$	$4.4850e-03$	-	-	
	PPSO [52]	-	-	$1.7267e-02$	$6.6415e-04$	-	-	
	FPA [55]	$7.8425e-04 \pm -$	$1.0312e-03$	$1.7298e-02$	$6.6531e-04$	$1.6873e-05$	-	
	MPSO [39]	$9.8247e-04 \pm -$	$1.2919e-03$	-	-	-	-	

(-) For the not available data in the corresponded paper

conditions as depicted in Figs. 8-9-10 for the studied three modules. The curves reveal the high qualified identified parameters by the MRUN as the most point of the AE curves of Figs. 8(c)-9(c)-10(c) are less than 0.02. Therefore the developed MRUN is recommended to provide efficient equivalent circuit parameters of the PV solar modules under different operating conditions.

VI. JUSTIFICATION UNDER PARTIAL SHADING AND VARIED TEMPERATURE CONDITIONS

The simulation implemented above and debates divulge the efficiency and accuracy of the extracted parameters for considered PV cells/panels under various operations cases. Thus, in this section, we are motivated to justify the recognized model parameters certainty in modeling connected strings with ($N \times 1, N$ is the number of series panels) and series-parallel arrays with ($N \times M$) panels under uniform and partially shaded operating conditions with considering temperature impact. For a brief, the data of the KC200GT PV panel is the established case in this section. The considered PV strings consist of three series (3S), six series (6S), and nine series (9S) PV modules. For the investigated arrays, three-dimensional arrays are recognized. The first array comprises 3S-2P PV modules where two

TABLE 7. The identified parameters by the proposed technique versus peers at different environmental conditions for 2D of Kyocera Solar (KC200GT) PV module.

		Parameters										
Cases/Alg		a_1	a_2	$R_s(\Omega)$	$R_p(\Omega)$	$I_{o1}(A)$	$I_{o2}(A)$	$I_{pv}(A)$	RMSE	$RMSE_{lambert}$	$Diff_{RMSE}$	AE_{MPP}
	MRUN	3.1737	1	0.33744	158.2578	$2.7875e-07$	$4.0577e-10$	8.225	0.0033228	0.0033228	0	0.18661
	RUN	1	1	0.33747	158.18	$1.0034e-12$	$4.0476e-10$	8.225	0.0033044	0.0033044	$-2.3683e-15$	0.18586
	AO	1.7202	4.4874	0.001	227.2339	$1e-05$	$1e-12$	8.2227	0.26863	0.26863	$-2.6978e-14$	2.7379
$1000W/m^2$	EFO	2.2402	1.3732	0.22405	237.1144	$3.2796e-06$	$2.5643e-07$	8.2391	0.06322	0.063089	-0.00013117	3.1192
$25\ ^\circ C$	BMO	3.2706	1.4411	0.20124	500	$1.0598e-07$	$5.9827e-07$	8.1857	0.061831	0.06183	$-6.1025e-07$	3.3473
	CapSA	1.4923	2.5426	0.18557	500	$1.0538e-06$	$8.9621e-08$	8.1938	0.068692	0.06869	$-2.0036e-06$	3.6643
	RFSO	4.387	1.7376	0.10952	482.4972	$1e-12$	$1e-05$	8.2113	0.10146	0.10146	$-6.3602e-13$	5.516
	MRUN	1.4514	1	0.33749	159.6622	$3.0479e-12$	$8.8695e-09$	8.3233	0.003248	0.003248	0	0.18394
	RUN	3.3014	1	0.33736	160.5313	$6.2371e-06$	$8.8679e-09$	8.3231	0.0033638	0.0033356	$-2.8223e-05$	0.18981
	AO	1.5518	1.1566	0.50298	188.8119	$1e-05$	$1e-12$	8.6572	0.41284	0.41284	$8.2723e-08$	12.2785
$1000W/m^2$	EFO	1.1238	5	0.28955	312.9407	$9.0191e-08$	$1e-12$	8.2872	0.028975	0.028975	$-1.1157e-12$	0.73182
$45\ ^\circ C$	BMO	1.153	4.9921	0.29019	285.2617	$1.3968e-07$	$1e-12$	8.2942	0.024155	0.024155	$-4.5267e-13$	1.332
	CapSA	1.2644	1.3413	0.22956	500	$1.4598e-11$	$1.7545e-06$	8.2881	0.048787	0.048787	$-6.3848e-09$	2.7987
	RFSO	4.5097	1.5114	0.17545	498.9273	$1e-12$	$1e-05$	8.3022	0.072759	0.072759	$-5.4473e-13$	4.234
	MRUN	1	1.0001	0.33677	163.9973	$4.7521e-07$	$6.5741e-10$	8.4702	0.0031905	0.0031905	0	0.12901
	RUN	1.7107	1.0008	0.33671	164.6902	$4.846e-08$	$4.8196e-07$	8.4701	0.0033237	0.0033217	$-1.9624e-06$	0.13938
	AO	3.8954	1.2888	0.6681	435.188	$1e-05$	$1e-05$	8.4176	0.4385	0.43852	$2.202e-05$	14.9789
$1000W/m^2$	EFO	1	1.7218	0.34214	165.3352	$4.661e-07$	$4.1667e-06$	8.474	0.010149	0.010283	0.00013485	0.34699
$75\ ^\circ C$	BMO	2.857	1	0.33678	164.2917	$1e-12$	$4.7587e-07$	8.47	0.0031909	0.0031909	$-2.3452e-12$	0.12777
	CapSA	5	1.0003	0.33644	170.7729	$5.7728e-06$	$4.7945e-07$	8.4677	0.0035976	0.0035959	$-1.667e-06$	0.090542
	RFSO	2.1326	1.2206	0.25824	430.4679	$1e-12$	$1e-05$	8.4437	0.033116	0.033116	$-7.3806e-12$	1.4254

8.8605e-9,8.3233

where $Diff_{RMSE}$ is equalled to ($RMSE_{lambert}$ - RMSE of Eq. 6).

TABLE 8. The identified parameters by the proposed technique versus peers at different environmental conditions for 2D of Sharp NU-(Q250W2) PV module.

		Parameters										
Cases/Alg		a_1	a_2	$R_s(\Omega)$	$R_p(\Omega)$	$I_{o1}(A)$	$I_{o2}(A)$	$I_{pv}(A)$	RMSE	$RMSE_{lambert}$	$Diff_{RMSE}$	AE_{MPP}
	MRUN	1	4.9804	0.33236	160.7042	$2.227e-10$	$5.9519e-06$	8.9182	0.00024395	0.00024395	0	0.016279
	RUN	1	1	0.33242	160.5059	$5.8294e-11$	$1.644e-10$	8.9183	0.00021564	0.00021564	$-4.5864e-16$	0.01358
	AO	2.857	1.7971	0.001	321.3092	$1e-05$	$1e-05$	8.8297	0.38487	0.38487	$5.5633e-07$	2.2856
$1000W/m^2$	EFO	1.2464	1	0.26141	467.0658	$2.7865e-08$	$1e-12$	8.8637	0.039831	0.039825	$-6.0774e-06$	2.0745
$25\ ^\circ C$	BMO	5	1.4817	0.17421	500	$1e-12$	$6.516e-07$	8.8804	0.069087	0.069087	$-7.9335e-13$	4.3488
	CapSA	5	1.5865	0.14474	500	$1e-05$	$1.9255e-06$	8.8896	0.08431	0.084306	$-4.5089e-06$	5.5256
	RFSO	2.7204	1.7755	0.082327	490.2885	$1e-12$	$1e-05$	8.9048	0.11129	0.11129	$-5.9137e-12$	7.2304
	MRUN	3.602	1.0007	0.33221	161.4772	$5.0866e-06$	$2.2205e-08$	9.1155	0.00037118	0.00037118	0	0.02043
	RUN	3.2624	1.0019	0.33164	162.2512	$7.6673e-06$	$2.2748e-08$	9.1152	0.00059941	0.00057425	$-2.5159e-05$	0.034164
	AO	4.0302	1.4257	0.34267	240.848	$2.6545e-06$	$7.3825e-06$	9.1496	0.22432	0.22432	$3.6361e-06$	11.2505
$1000W/m^2$	EFO	1.2377	5	0.24784	461.9065	$1.0203e-06$	$1e-12$	9.0721	0.035395	0.035395	$-5.8649e-13$	1.5651
$55\ ^\circ C$	BMO	2.6169	1.2526	0.24828	440.828	$1e-12$	$1.2203e-06$	9.0744	0.035353	0.035353	$-6.9022e-12$	1.9105
	CapSA	1.3038	5	0.2308	500	$2.2783e-06$	$1e-12$	9.0747	0.042255	0.042255	$-3.3792e-13$	2.3659
	RFSO	4.4717	1.4436	0.1834	486.3965	$1e-12$	$1e-05$	9.087	0.062837	0.062837	$-4.3313e-13$	3.756
	MRUN	3.7626	1	0.33234	160.6908	$1.8572e-07$	$1.6232e-07$	9.2146	0.0002077	0.0002077	0	0.010132
	RUN	1.0001	1.0425	0.3318	161.376	$1.574e-07$	$1.0603e-08$	9.2143	0.00043355	0.00042811	$-5.4365e-06$	0.021108
	AO	1.14	4.3192	0.60498	264.9285	$9.1739e-07$	$4.9712e-06$	9.2621	0.3527	0.35271	$8.6401e-06$	13.9985
$1000W/m^2$	EFO	2.6999	1.1097	0.30025	365.9153	$1e-05$	$9.5114e-07$	9.1743	0.019283	0.019289	$5.8126e-06$	0.85074
$70\ ^\circ C$	BMO	1	5	0.33231	160.2617	$1.6226e-07$	$1.0452e-07$	9.2148	0.00023205	0.00023199	$-6.095e-08$	0.012311
	CapSA	5	1.1823	0.27086	488.25	$6.8271e-08$	$2.5979e-06$	9.1723	0.026921	0.026921	$-1.1032e-08$	1.34
	RFSO	1.2973	3.4052	0.22553	461.2318	$1e-05$	$1e-12$	9.1834	0.044013	0.044013	$-1.0313e-12$	2.3088

where $Diff_{RMSE}$ is equalled to ($RMSE_{lambert}$ - RMSE of Eq. 6).

TABLE 9. The identified parameters by the proposed technique versus peers at different environmental conditions for 2D of Pythagoras Solar Large PVGU Window.

		Parameters										
Cases/Alg		a_1	a_2	$R_s(\Omega)$	$R_p(\Omega)$	$I_{o1}(A)$	$I_{o2}(A)$	$I_{pv}(A)$	RMSE	$RMSE_{lambert}$	$Diff_{RMSE}$	AE_{MPP}
	MRUN	1	1.5159	0.49484	394.8694	$6.9199e-11$	$1.7116e-12$	6.0054	0.0028506	0.0028506	0	0.2506
	RUN	1.0088	1.2746	0.47015	490.3654	$7.5961e-11$	$1.9785e-09$	5.9951	0.0087954	0.0085604	-0.00023498	0.64655
	AO	3.9998	1.903	0.001	142.8736	$1e-05$	$1e-05$	5.994	0.25886	0.25886	$1.3913e-08$	25.3983
$1000W/m^2$	EFO	1.6198	1	0.079606	500	$1.0627e-06$	$1e-12$	6.0198	0.075503	0.075471	$-3.2504e-05$	8.0507
$25\ ^\circ C$	BMO	1.6036	5	0.062428	500	$9.3552e-07$	$1e-12$	6.0183	0.072521	0.072521	$-1.5475e-13$	7.5697
	CapSA	1	2.6361	0.47435	500	$7.0947e-11$	$1.7505e-06$	5.9931	0.014044	0.013788	-0.00025619	0.40604
	RFSO	1.8945	2.8988	0.001	435.0821	$1e-05$	$1e-12$	6.0656	0.12732	0.12732	$1.2795e-14$	12.6335
	MRUN	3.1473	1	0.49485	394.4676	$2.9273e-08$	$7.2097e-10$	5.8798	0.0026777	0.0026777	0	0.27901
	RUN	1.0045	1.4456	0.49111	398.2744	$7.9807e-10$	$1e-12$	5.8792	0.0031621	0.0031621	$-9.0095e-09$	0.32484
	AO	1.7136	2.0714	0.001	350.3254	$1e-05$	$1e-12$	6.0471	0.14451	0.14451	$-2.6867e-14$	4.8553
$1000W/m^2$	EFO	1.1745	2.0346	0.31977	229.7853	$2.0517e-08$	$4.122e-06$	5.9541	0.049665	0.049231	-0.00043331	4.1619
$40\ ^\circ C$	BMO	1	1.4301	0.17757	500	$1e-12$	$7.0424e-07$	5.8855	0.050287	0.050281	$-6.0231e-06$	5.709
	CapSA	4.2949	1.1812	0.37721	500	$4.3021e-06$	$2.3776e-08$	5.8722	0.024642	0.024644	$1.6742e-06$	2.8275
	RFSO	1.7935	1.7157	0.001	497.2074	$1e-12$	$1e-05$	5.9007	0.081854	0.081854	$-1.7514e-14$	9.4445
	MRUN	1	4.9884	0.49315	399.408	$1.1914e-08$	$1.6874e-07$	5.7114	0.0025875	0.0025875	0	0.25355
	RUN	1.3644	1.0006	0.49303	400.7105	$1.7053e-12$	$1.2053e-08$	5.7113	0.0026521	0.0026521	$-2.7121e-09$	0.2631
	AO	5	1.534	0.57828	190.5732	$1e-12$	$1e-05$	5.9642	0.23205	0.23205	$7.308e-13$	10.8888
$1000W/m^2$	EFO	1.2212	5	0.30759	500	$4.5426e-07$	$1e-12$	5.7074	0.02743	0.02743	$-4.0037e-13$	2.8687
$60\ ^\circ C$	BMO	3.9316	1.3182	0.23315	499.678	$1.7723e-07$	$1.5044e-06$	5.7141	0.037671	0.037671	$-8.7914e-08$	3.7947
	CapSA	1.1028	1.7714	0.31234	500	$6.581e-08$	$1e-05$	5.7134	0.039672	0.039406	-0.00026599	1.6003
	RFSO	1.506	3.2803	0.07799	467.7994	$1e-05$	$1e-12$	5.7271	0.059411	0.059411	$-3.5804e-13$	5.6252

where $Diff_{RMSE}$ is equalled to ($RMSE_{lambert}$ - RMSE of Eq. 6).

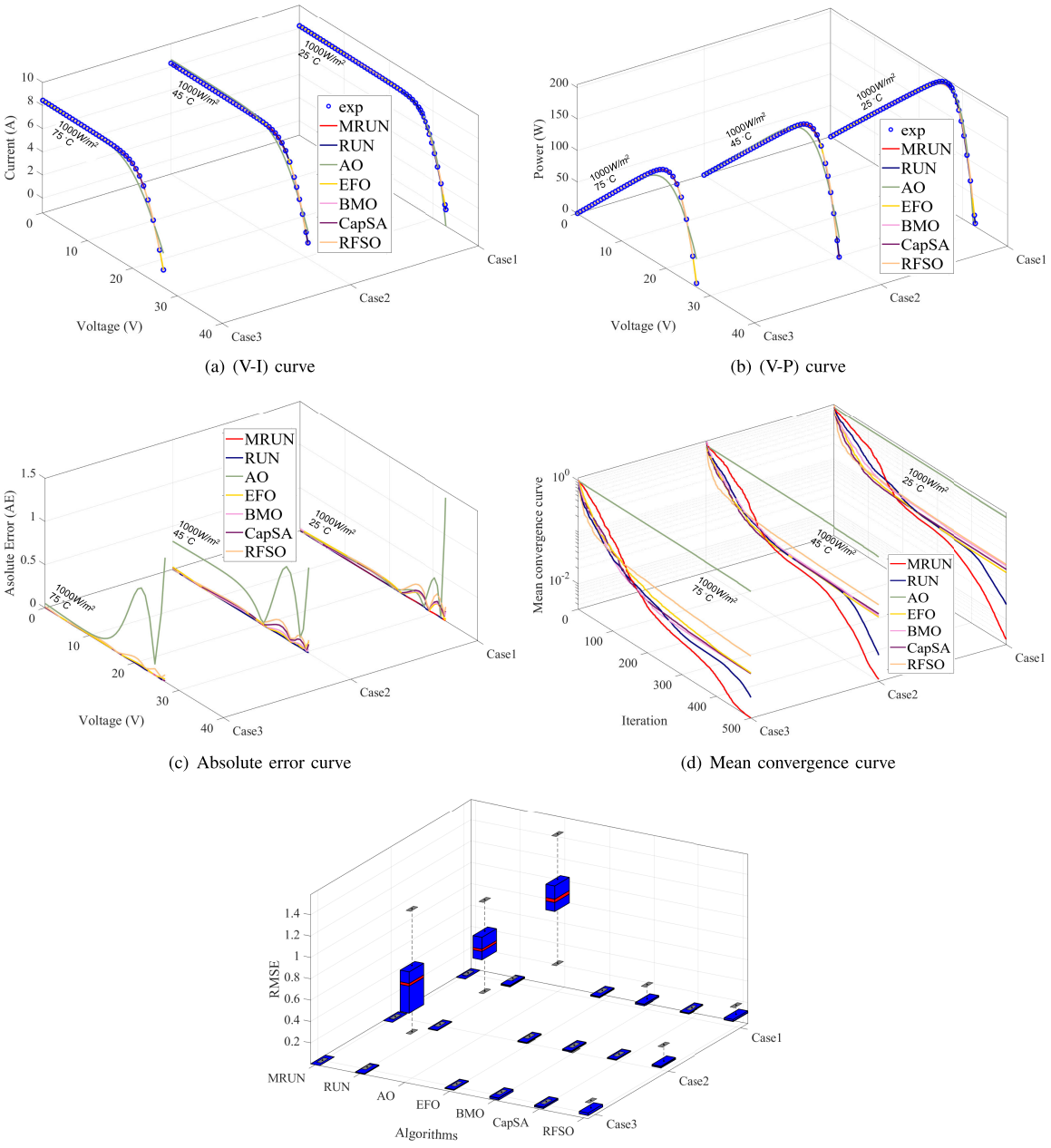

(a) (V-I) curve

(b) (V-P) curve

(c) Absolute error curve

(d) Mean convergence curve

(e) RMSE values

FIGURE 5. The implemented optimizers responses in case of 2D model of Kyocera Solar (KC200GT) PV module throughout 25 separate runs.

parallel strings (2P) have three series modules in each string (3S). The second array consists of 6 series-3 parallel (6S-3P) PV modules, and the third one has 9 series-9 parallel (9S-9P) PV panels. The described series of experiments are listed in Table 11.

A. MATHEMATICAL FORMULATION FOR THE CURRENT, VOLTAGE AND POWER OF THE PV ARRAY

In this part, the strategies that followed in computing the string and SP interconnected arrays current and voltage under PS conditions are represented as follows:

- In the first step, the parameters of the used PV equivalent circuit (1D or 2D) are identified at SOC. Under the different operating conditions, those parameters are normalized using equations of Section II. By this way, the V-I curves of the PV module are computed for the corresponding operating conditions.
- For the string current and voltage values, suppose having a string with connected three modules receive three different levels of radiations that are $900W/m^2$, $400W/m^2$, $100W/m^2$ as shown in Fig. 11(a). The V-I and V-P characteristics of each module in the

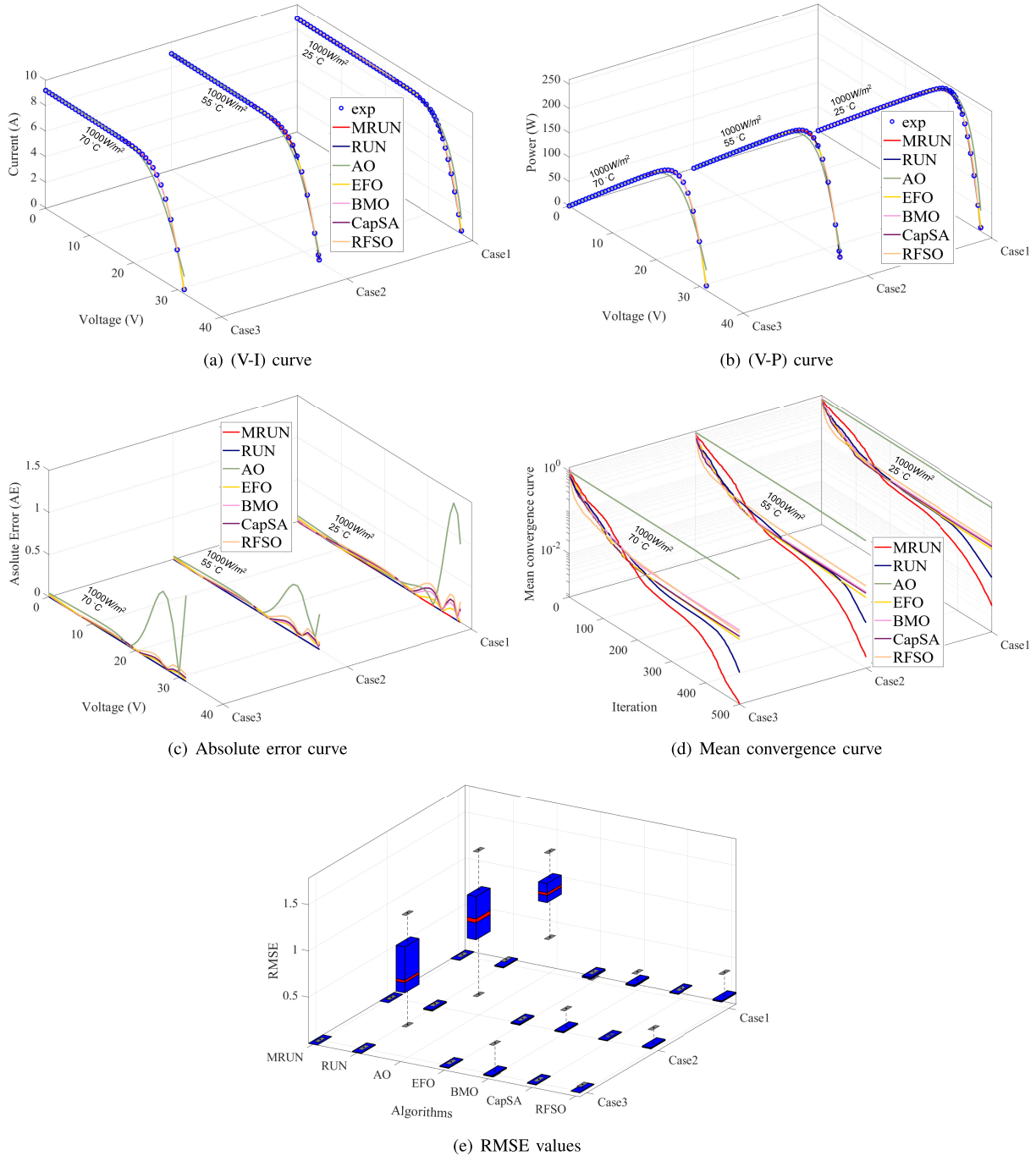

(a) (V-I) curve

(b) (V-P) curve

(c) Absolute error curve

(d) Mean convergence curve

(e) RMSE values

FIGURE 6. **The implemented optimizers responses in case of 2D model of Sharp NU-(Q250W2) PV module throughout 25 separate runs.**

string are plotted in Fig. 11(b), it's obvious that the modules currents levels are varied because of the PS. The series connection between these modules in a string as in Fig. 11(a) with bypass diode and blocking diode generates V-I, V-P characteristics with three levels (ladder shape) as in Fig. 11(c). To understand the strategy that followed to conducting these laddered characteristics, the following steps are reported.

– For zone 1 of Fig. 12(a), the current of M2 and M3 is lower than that of M1 as illustrated in Fig. 11(b). Then, the M1 current is the dominant in this zone while the other modules are bypassed. The current of the bypassed modules flow through their parallel diodes (conducting links are appeared by red line), as illustrated in Fig.12(a). Thus the current of the string in this zone is controlled by the condition of $I_{SC_{M2}} \leq I_{str_{Zone1}} < I_{SC_{M1}}$. The corresponding

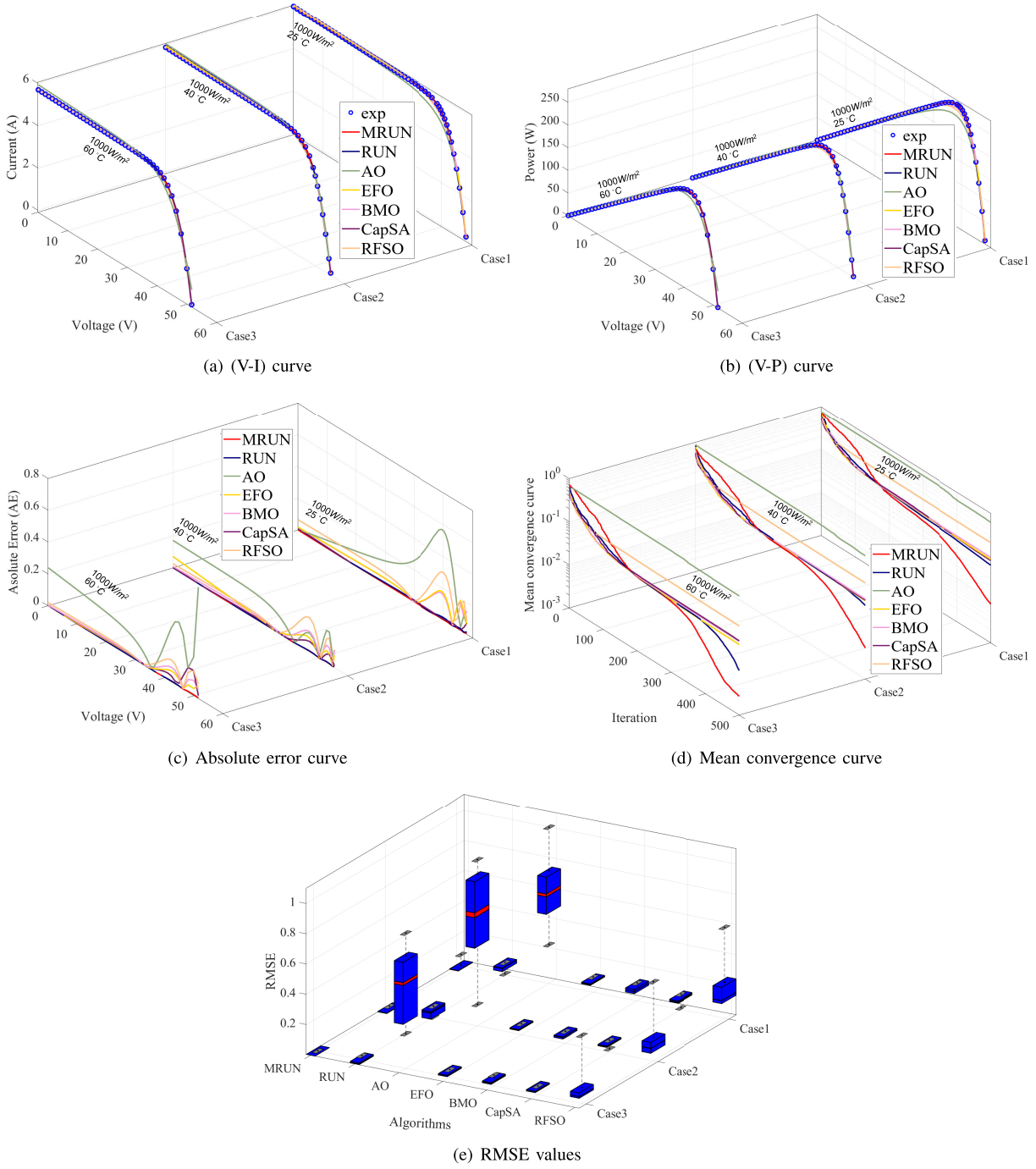

(a) (V-I) curve

(b) (V-P) curve

(c) Absolute error curve

(d) Mean convergence curve

(e) RMSE values

FIGURE 7. The implemented optimizers responses in case of 2D model of Pythagoras Solar Large PVGU Window throughout 25 separate runs.

voltage of the string in this zone is calculated by Eq.(ps1).

$$V_{str_{Zone1}} = V_{M1} + V_{Bypassdiode2} + V_{Bypassdiode3} + V_{Blockingdiode} \quad (29)$$

where $V_{str_{Zone1}}$ is the voltage of the string of Zone 1, V_{M1} is the first module voltage, and the $V_{Bypassdiode2}$ and $V_{Bypassdiode3}$ are the voltage values of the parallel-connected bypass diodes of the second and third modules, respectively. Finally, the $V_{Blockingdiode}$ refers to the voltage of the blocking diode. The voltage drop V_D across the diode can be computed using Eq.30.

$$V_D = V_{fwd} + R \times I_D \quad (30)$$

where V_D is an implementation to the $V_{Bypassdiode2}$, $V_{Bypassdiode3}$ and $V_{Blockingdiode}$. The V_{fwd} symbolizes to the diode forward voltage, the R refers to the

TABLE 10. Statistical metrics for the obtained results by MRUN versus the basic RUN during handling the 1D and 2D models of the studied PV modules.

			Statically metrics						Wilcoxon signed-rank test MRUN vs RUN			
Module/Cases/Alg			Best	Worst	Average	Median	Variance	Std	R_+	R_-	p_{value}	h_o
KC200GT	Case 1	MRUN	0.0033228	0.011021	0.0041417	0.0037025	2.3813e-06	0.0015431	-	-	-	-
		RUN	0.0033044	0.044287	0.019501	0.019229	0.00012138	0.011017	322	3	1.7735e-05	1
	Case 2	MRUN	0.003248	0.0079916	0.0035505	0.0032808	8.9899e-07	0.00094815	-	-	-	-
		RUN	0.0033638	0.020159	0.010455	0.011444	1.9274e-05	0.0043902	318	7	2.8639e-05	1
	Case 3	MRUN	0.0031905	0.0043235	0.0032489	0.003199	5.0411e-08	0.00022452	-	-	-	-
		RUN	0.0033237	0.024274	0.0081485	0.0072423	2.4334e-05	0.0049329	325	0	1.229e-05	1
NU-(Q250W2)	Case 1	MRUN	0.00024395	0.0092783	0.0038393	0.0036945	6.8264e-06	0.0026127	-	-	-	-
		RUN	0.00021564	0.052333	0.018713	0.017971	0.00012152	0.011024	317	8	3.2229e-05	1
	Case 2	MRUN	0.00037118	0.0040551	0.0016557	0.0014549	8.4985e-07	0.00092187	-	-	-	-
		RUN	0.00059941	0.0262	0.011227	0.011473	5.0829e-05	0.0071295	317	8	3.2229e-05	1
	Case 3	MRUN	0.0002077	0.0043312	0.00089384	0.0005465	7.6256e-07	0.00087325	-	-	-	-
		RUN	0.00043355	0.012837	0.0052932	0.0048524	1.2799e-05	0.0035776	313	12	5.1329e-05	1
PVGU Window	Case 1	MRUN	0.0028506	0.078659	0.0078881	0.0042838	0.00022332	0.014944	-	-	-	-
		RUN	0.0087954	0.082565	0.063315	0.07853	0.00066823	0.02585	322	3	1.7735e-05	1
	Case 2	MRUN	0.0026777	0.017787	0.0052532	0.0033881	1.6035e-05	0.0040044	-	-	-	-
		RUN	0.0031621	0.075322	0.05094	0.063375	0.00070666	0.026583	322	3	1.7735e-05	1
	Case 3	MRUN	0.0025875	0.0039985	0.002743	0.0026123	1.191e-07	0.00034511	-	-	-	-
		RUN	0.0026521	0.029806	0.010849	0.007679	7.3667e-05	0.008583	316	9	3.6243e-05	1

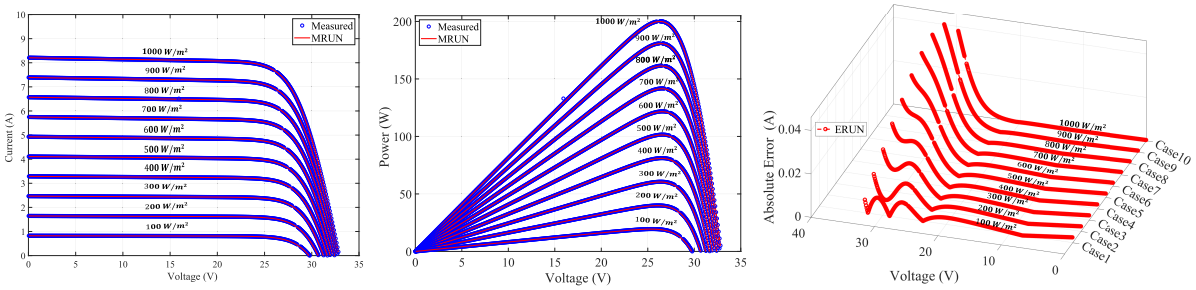

(a) V-I curve (b) V-P curves (c) absolute error (AE) curves

FIGURE 8. The performance of estimated parameters by MRUN for Kyocera Solar (KC200GT) module at various irradiation.

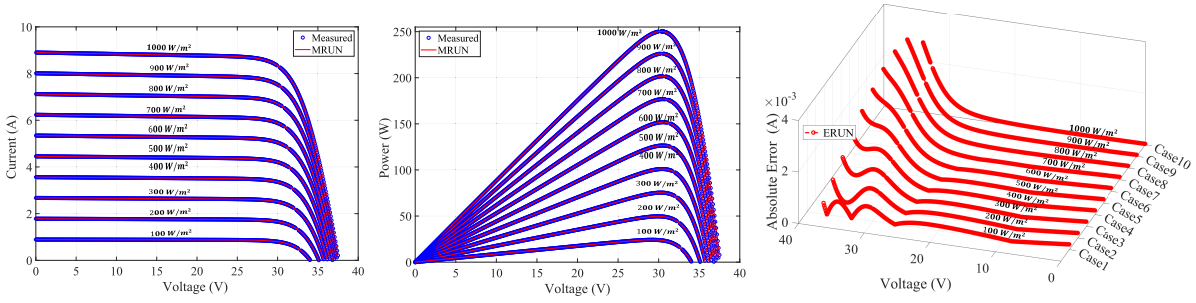

(a) V-I curve (b) V-P curve (c) AE curve

FIGURE 9. The performance of estimated parameters by MRUN forSharp NU-(Q250W2) PV module at various irradiation.

diode equivalent resistance in the conducing mode and the I_D is the current flows through the diode. For the ideal diode the V_{fwd} and R are equaled 0.

– For Zone 2 of Fig.12(b), M3 is generating a lower current than that of the other modules (M1 and M2) as illustrated in Fig.11(b). Thus, the currents of the M1 and M2 are the dominant ones in this zone; in contrast, the M3 is bypassed. Thus, the current of this zone is controlled by the condition of $I_{SC_{M3}} \leq I_{str_{Zone2}} \leq I_{SC_{M2}}$. The corresponding voltage of the string in this zone is expressed as follows:

$$V_{str_{Zone2}} = V_{M1} + V_{M2} + V_{Bypassdiode3} + V_{Blockingdiode} \quad (31)$$

– For Zone 3 of Fig. 12(c), the three modules of the string (M1,2,3) are generating currents (the conducting elements are colored in red). Thus the

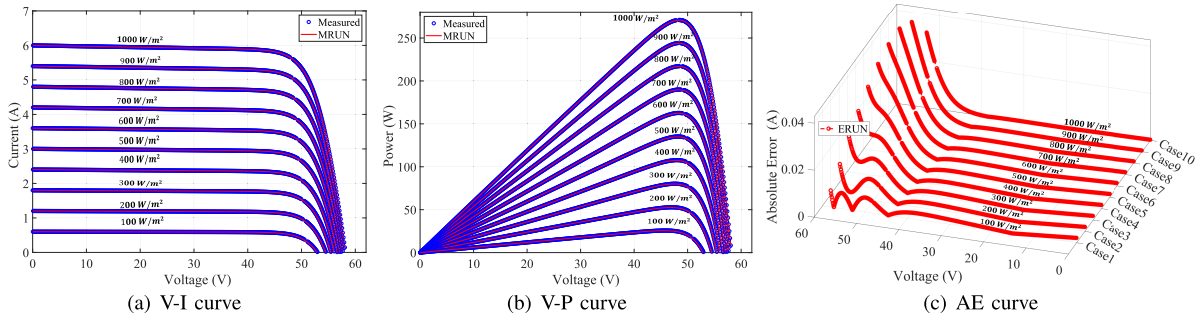

FIGURE 10. The performance of estimated parameters by MRUN for Pythagoras Solar Large PVGU Window at various irradiation.

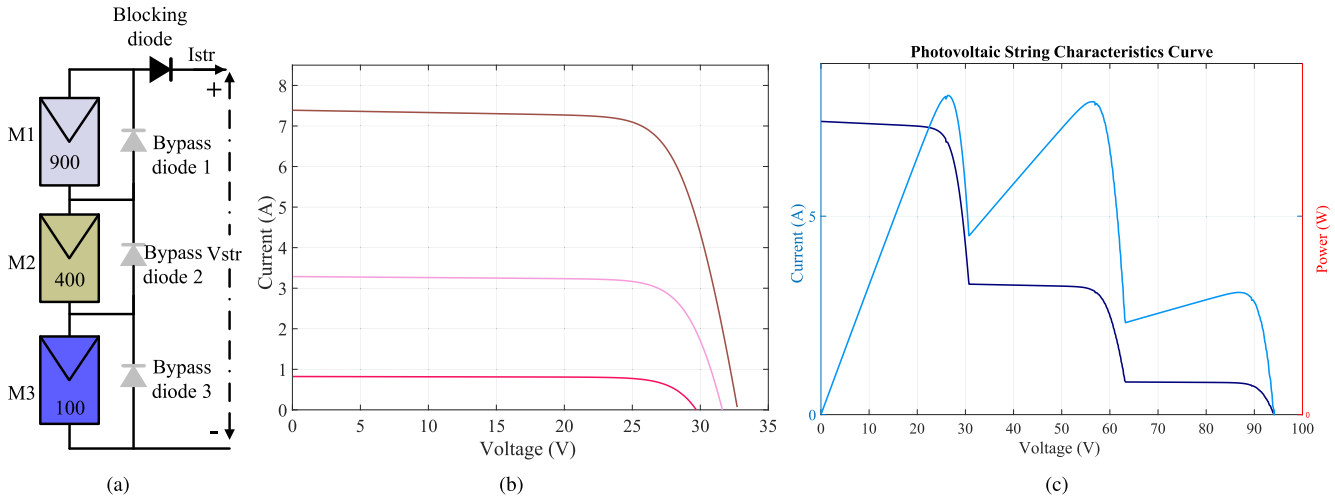

FIGURE 11. The 3 × 1 string under PS: (a) String pattern, (b) V-I curves of shaded module, and (c) V-I, V-P curves of the total string.

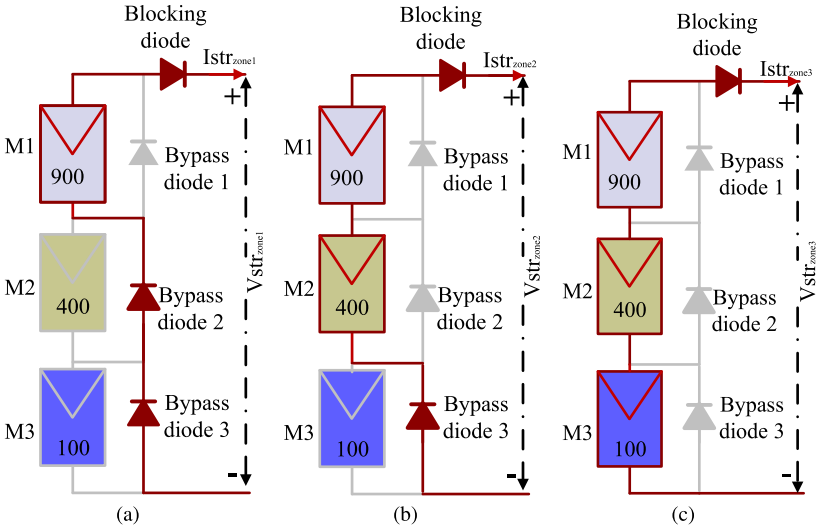

FIGURE 12. The operation of the 3 × 1 string through the three zones (a) Zone 1: M1 generates current and M2, M3 are bypassed, (b) Zone 2: M1, M2 generate current and M3 is bypassed, and (c) Zone 3: M1, M2, M3 generate current.

TABLE 11. The considered scenarios and systems.

	Varied radiation and 25 $^{\circ}C$						Varied radiation and temperature		
	PV string				PV array				
Cond	3S	6S	9S	3S-2P	6S-3P	9S-9P	6S	3S-2P	6S-3P
Scenario 1	$1000W/m^2$ for all modules	$1000W/m^2$ for all modules	$1000W/m^2$ for all modules	$1000W/m^2$ for all modules	$1000W/m^2$ for all modules	$1000W/m^2$ for all modules			
Scenario 2	M1, M2, M3 $1000W/m^2$, $600W/m^2$, $200W/m^2$	M1, M2, M3, M4, M5, M6 $1000W/m^2$, $1000W/m^2$, $1000W/m^2$, $300W/m^2$, $300W/m^2$, $300W/m^2$	M1, M2, M3, M4, M5, M6, M7, M8, M9 $1000W/m^2$, $1000W/m^2$, $1000W/m^2$, $700W/m^2$, $700W/m^2$, $700W/m^2$, $100W/m^2$, $100W/m^2$, $100W/m^2$	Str1, Str2 $1000W/m^2$, $550W/m^2$, $250W/m^2$	Str1-SStr6 $1000W/m^2$, $1000W/m^2$, $750W/m^2$, $750W/m^2$ $350W/m^2$, $350W/m^2$	Str1-Str9 first five rows $900W/m^2$, 6^{th}, 7^{th} rows are $600W/m^2$, 8^{th}, 9^{th} rows are $400W/m^2$	M1, M2, M3, M4, M5, M6 $1000W/m^2$, $1000W/m^2$, $1000W/m^2$ with 25 $^{\circ}C$, $300W/m^2$, $300W/m^2$, $300W/m^2$ with 75 $^{\circ}C$	Str1, Str2 $1000W/m^2, 25\ ^{\circ}C$, $550W/m^2$, $250W/m^2$ with 45 $^{\circ}C$	Str1-Str6 $1000W/m^2$, $1000W/m^2$ $25\ ^{\circ}C$, $750W/m^2$, $750W/m^2, 45\ ^{\circ}C$, $350W/m^2$, $350W/m^2, 75\ ^{\circ}C$

where M_i symbols to the i^{th} module, Str_i refers to a i^{th} string, S and P for series and parallel connections.

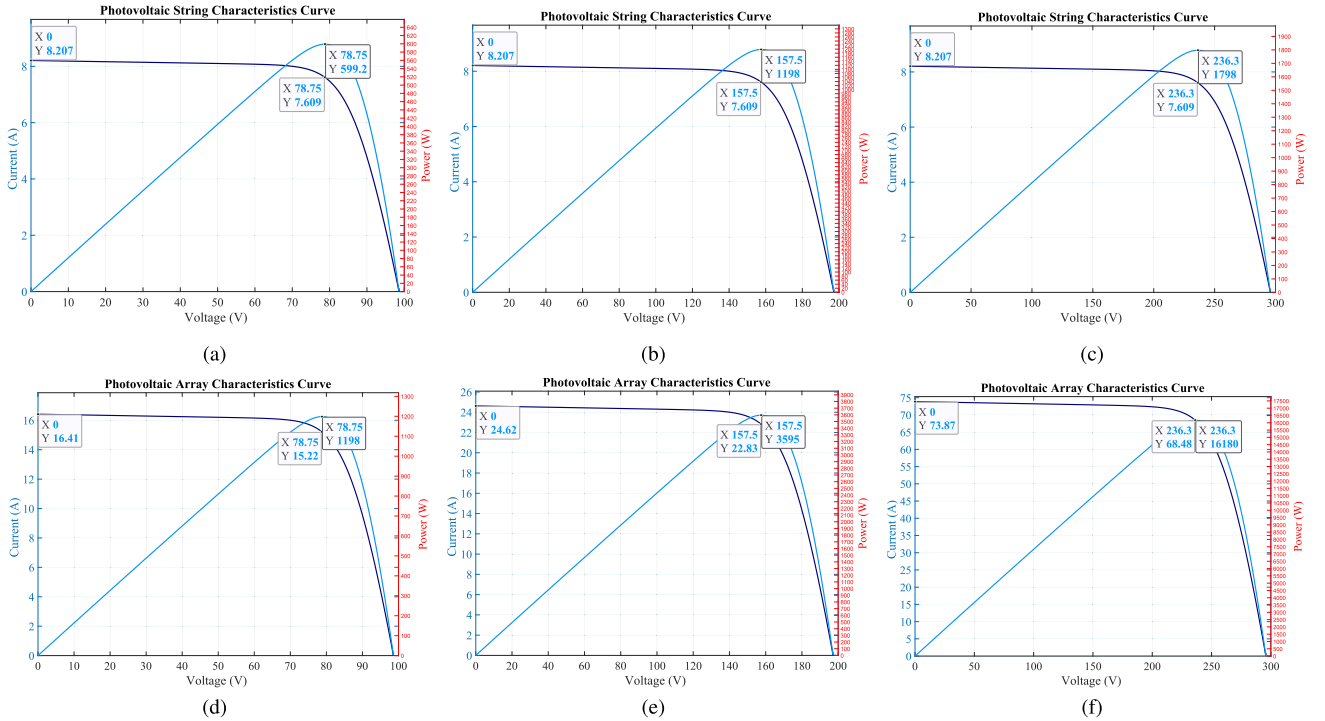

FIGURE 13. The PV system characteristics at scenarios 1 for (a) 3 × 1 string, (b) 6 × 1 string, (c) 9 × 1 string, (d) 3 × 2 array, (e) 6 × 3 array, and (f) 9 × 9 array at uniform irradiation condition.

current of the string in this zone is controlled by the rule of $0 \leq I_{str_{Zone3}} \leq I_{SC_{M3}}$ accordingly, the string voltage can be modeled through Eq.33.

$$V_{str_{Zone3}} = V_{M1} + V_{M2} + V_{M3} + V_{Blockingdiode} \tag{32}$$

The total harvested string power (P_{str}) is computed by multiplying the string voltage and current as reported in Eq. 33.

$$P_{str} = V_{str} \times I_{str} \tag{33}$$

- To compute the voltage and current of the whole array composed of M parallel strings, the previously described steps are conducted for each string. Then, the current and voltage of the array are calculated as follows.

$$I_{array} = I_{str1} + I_{str2} + \ldots I_{strM} \tag{34a}$$

$$V_{oc_{array}} = max(V_{oc_{str1}}, V_{oc_{str2}}, \ldots V_{oc_{strM}}) \tag{34b}$$

where I_{array} and $V_{oc_{array}}$ are the array current and open circuit voltage, respectively, the $V_{oc_{str1}}$ is the voltage of string M at open circuit.

B. CASE STUDY: KYOCERA SOLAR (KC200GT)

This part presents a case study for implementing the V-I and V-P characteristics of Kyocera Solar (KC200GT) based on the module identified parameters of section V-B by MRUN. Fig. 13 shows the V-I and V-P characteristics of the KC200GT PV interconnected strings and arrays under uniform irradiation levels. The highlighted values of current, voltage, and power at short circuit point and maximum power one are illustrated in Fig.13(a) illustrate the high certainty of the identified model parameters that conducted to detect the short circuit and maximum power current, voltage, and

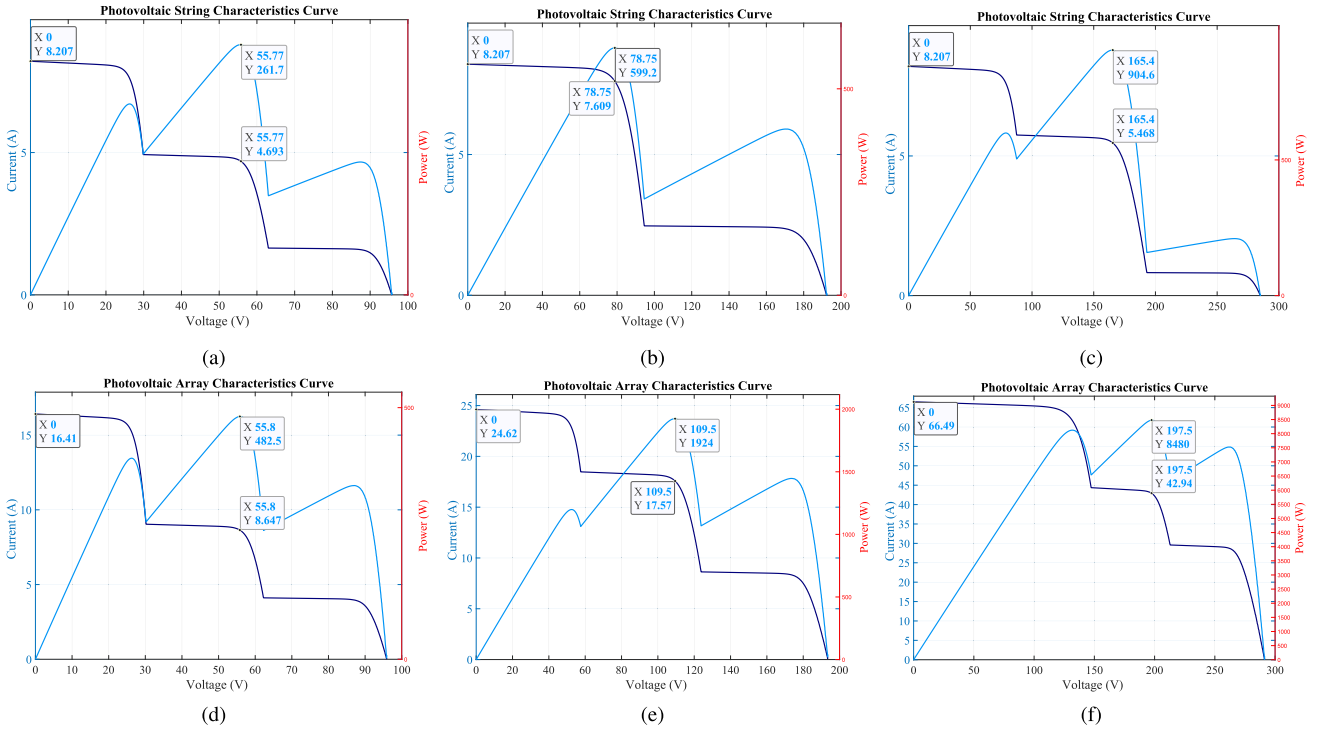

FIGURE 14. The PV system characteristics at scenarios 2 for (a) 3 × 1 string, (b) 6 × 1 string, (c) 9 × 1 string, (d) 3 × 2 array, (e) 6 × 3 array, and (f) 9 × 9 array at at PS (variation of radiation and 25 °C).

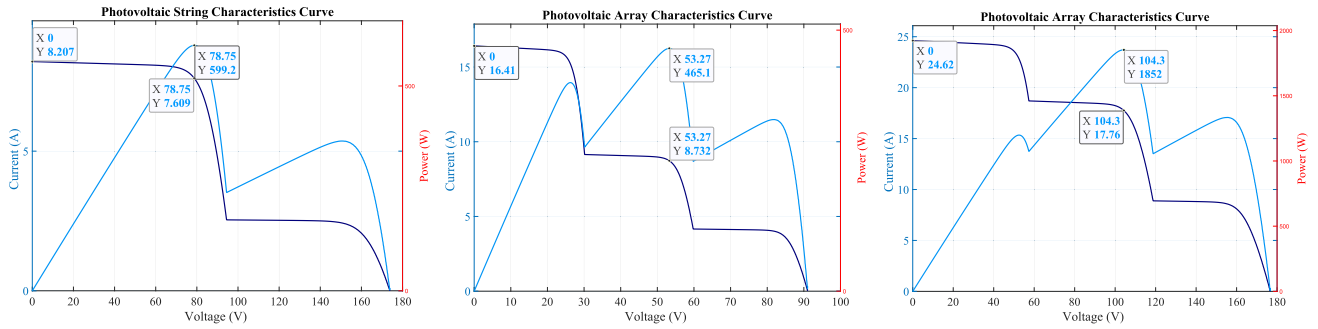

FIGURE 15. The PV system characteristics at different levels of radiation and temperature for (a) 6 × 1 string with 25, 75 °C, (b) 3 × 2 array with 25, 45, 45 °C, respectively for each module in the string, and (c) 6 × 3 array with 25, 25, 45, 45, 75, 7 °C, with PS.

power with nearly 99.9% accuracy as the expected and detected values of the short circuit and maximum current are (8.21 (A), 7.61 (A)), and (8.207 (A), 7.609 (A)) respectively. The expected value of the string voltage at the maximum power point is nearly equal to the summation of the voltage of the three modules that is nearly equal to 78.9 (3*26.3). The detected value of the voltage is 78.75 that is about 99.8% from the expected value. The accuracy of the identified parameters by MRUN is also affirmed from the figures of the 6×1 string, 9×1 string, and the considered arrays as shown in Fig. 13. For the non-uniform incident irradiation condition of Fig.14, the V-I and V-P characteristics are highly matched with the calculated current, voltage, and power based on equations of Section VI-A. For fig.15(a), a 3×1 string is subjected to three different radiations levels of $1000W/m^2$, $600W/m^2$, $200W/m^2$, accordingly the PV string characteristics has three ladders. The first ladder of the characteristics is controlled by the current of M1 that is subjected to $1000W/m^2$ until the flowing current becomes equal to the generates current of M2 (600/1000 * 8.21 = 4.9260); in this step, the M2 current is the dominant one, and finally, M1 generated current (100/1000 * 8.21 = 1.6420) becomes the dominant one. The output voltage is the summation of the three modules voltage. The displayed curves of Fig. 14 are closely matched with these calculations that approve the accuracy of the identified parameters. For considering the change in the temperature

and irradiation, the characteristics of PV string and arrays are exhibited in Fig. 15. Based on the previous discussions and observations, the MRUN is a recommended optimizer for identifying the 1D and 2D PV models parameters.

VII. CONCLUSION

Providing efficient PV solar cell/module modeling is the first essential step before the system installation. Therefore, this paper proposed an interactive modified version of an algorithm based on runge kutta optimizer (MRUN). The proposed algorithm performance has been enhanced to identify the PV single (1D) and double (2D) diode models parameters using several solar cells/modules datasets. The MRUN results have been validated through intensive comparisons with recent meta-heuristic optimization algorithms, including basic RUN, aquila optimizer (AO), electric fish optimizer (EFO), barnacles mating optimizer (BMO), capuchin search algorithm (CapSA), red fox optimization algorithm (RFSO) moreover recent twenty-five state-of-the-art-techniques from literature. The power-voltage (V-P), voltage-current (V-I) characteristics, the absolute error between the estimated and measured datasets, the mean convergence curves, and the fitness function (RMSE throughout a set of separate runs are utilized for the comparison purpose. Furthermore, a group of statistical metrics and non-parametric analysis of the Wilcoxon signed-rank test have been computed. The comparisons and analyses reveal the quality enhancements achieved via applying the proposed RUN optimizer in identifying the PV modules parameters compared to the basic Run optimizer and other recent state-of-the-art techniques. The accuracy, consistency, and convergence properties of the proposed optimizer are remarkable points in the results. The efficiency of the extracted parameters has been justified in modeling large interconnected solar systems in series, parallel or series-parallel schemes; several sizes of strings and PV arrays have been considered under several operating conditions of temperature and radiation. The attained V-P and V-I characteristics of the studied strings and arrays divulge the efficient emulating for the physical performance of the considered systems.

For future work, the authors will apply the proposed optimizer for maximum power point tracking optimization problem and other engineering applications.

CONFLICT OF INTEREST

The authors declare there is no conflict of interest.

REFERENCES

[1] R. Chenouard and R. A. El-Sehiemy, "An interval branch and bound global optimization algorithm for parameter estimation of three photovoltaic models," *Energy Convers. Manage.*, vol. 205, Feb. 2020, Art. no. 112400.

[2] L. Sandrolini, M. Artioli, and U. Reggiani, "Numerical method for the extraction of photovoltaic module double-diode model parameters through cluster analysis," *Appl. Energy*, vol. 87, no. 2, pp. 442–451, Feb. 2010.

[3] X. Gao, Y. Cui, J. Hu, G. Xu, and Y. Yu, "Lambert W-function based exact representation for double diode model of solar cells: Comparison on fitness and parameter extraction," *Energy Convers. Manage.*, vol. 127, pp. 443–460, Nov. 2016.

[4] M. H. Qais, H. M. Hasanien, S. Alghuwainem, and A. S. Nouh, "Coyote optimization algorithm for parameters extraction of three-diode photovoltaic models of photovoltaic modules," *Energy*, vol. 187, Jan. 2019, Art. no. 116001.

[5] N. Hamid, R. Abounacer, M. I. Oumhand, M. Feddaoui, and D. Agliz, "Parameters identification of photovoltaic solar cells and module using the genetic algorithm with convex combination crossover," *Int. J. Ambient Energy*, vol. 40, no. 5, pp. 517–524, Jul. 2019.

[6] S. Li, W. Gong, X. Yan, C. Hu, D. Bai, L. Wang, and L. Gao, "Parameter extraction of photovoltaic models using an improved teaching-learning-based optimization," *Energy Convers. Manage.*, vol. 186, pp. 293–305, Oct. 2019.

[7] D. Yousri, M. Abd Elaziz, D. Oliva, L. Abualigah, M. A. Al-Qaness, and A. A. Ewees, "Reliable applied objective for identifying simple and detailed photovoltaic models using modern metaheuristics: Comparative study," *Energy Convers. Manage.*, vol. 223, Nov. 2020, Art. no. 113279.

[8] A. R. Jordehi, "Parameter estimation of solar photovoltaic (PV) cells: A review," *Renew. Sustain. Energy Rev.*, vol. 61, pp. 354–371, Oct. 2016.

[9] M. H. Hassan, S. Kamel, L. Abualigah, and A. Eid, "Development and application of slime mould algorithm for optimal economic emission dispatch," *Expert Syst. Appl.*, vol. 182, Nov. 2021, Art. no. 115205.

[10] V. J. Chin, Z. Salam, and K. Ishaque, "Cell modelling and model parameters estimation techniques for photovoltaic simulator application: A review," *Appl. Energy*, vol. 154, pp. 500–519, Sep. 2015.

[11] A. Youssef, M. El-Telbany, and A. Zekry, "The role of artificial intelligence in photo-voltaic systems design and control: A review," *Renew. Sustain. Energy Rev.*, vol. 78, pp. 72–79, Oct. 2017.

[12] G. Xiong, J. Zhang, D. Shi, and Y. He, "Parameter extraction of solar photovoltaic models using an improved whale optimization algorithm," *Energy Convers. Manage.*, vol. 174, pp. 388–405, Oct. 2018.

[13] L. Abualigah and A. Diabat, "Advances in sine cosine algorithm: A comprehensive survey," *Artif. Intell. Rev.*, vol. 54, pp. 2567–2608, Apr. 2021.

[14] L. Abualigah and A. Diabat, "A comprehensive survey of the grasshopper optimization algorithm: Results, variants, and applications," *Neural Comput. Appl.*, vol. 32, no. 19, pp. 15533–15556, 2020.

[15] K. Yu, J. J. Liang, B. Y. Qu, X. Chen, and H. Wang, "Parameters identification of photovoltaic models using an improved JAYA optimization algorithm," *Energy Convers. Manage.*, vol. 150, pp. 742–753, Oct. 2017.

[16] O. S. Elazab, H. M. Hasanien, I. Alsaidan, A. Y. Abdelaziz, and S. M. Muyeen, "Parameter estimation of three diode photovoltaic model using grasshopper optimization algorithm," *Energies*, vol. 13, no. 2, p. 497, Jan. 2020.

[17] M. Said, A. M. Shaheen, A. R. Ginidi, R. A. El-Sehiemy, K. Mahmoud, M. Lehtonen, and M. M. F. Darwish, "Estimating parameters of photovoltaic models using accurate turbulent flow of water optimizer," *Processes*, vol. 9, no. 4, p. 627, Apr. 2021.

[18] A. A. Ismaeel, E. H. Houssein, D. Oliva, and M. Said, "Gradient-based optimizer for parameter extraction in photovoltaic models," *IEEE Access*, vol. 9, pp. 13403–13416, 2021.

[19] M. Premkumar, P. Jangir, R. Sowmya, R. M. Elavarasan, and B. S. Kumar, "Enhanced chaotic JAYA algorithm for parameter estimation of photovoltaic cell/modules," *ISA Trans.*, vol. 116, pp. 139–166, Oct. 2021.

[20] Y. Xu, X. Kong, Y. Zeng, S. Tao, and X. Xiao, "A modeling method for photovoltaic cells using explicit equations and optimization algorithm," *Int. J. Electr. Power Energy Syst.*, vol. 59, pp. 23–28, Jul. 2014.

[21] J. Liang, S. Ge, B. Qu, K. Yu, F. Liu, H. Yang, P. Wei, and Z. Li, "Classified perturbation mutation based particle swarm optimization algorithm for parameters extraction of photovoltaic models," *Energy Convers. Manage.*, vol. 203, Jan. 2020, Art. no. 112138.

[22] I. A. Ibrahim, M. Hossain, B. C. Duck, and M. Nadarajah, "An improved wind driven optimization algorithm for parameters identification of a triple-diode photovoltaic cell model," *Energy Convers. Manage.*, vol. 213, 2020, Art. no. 112872.

[23] D. H. Wolper and W. G. Macready, "No free lunch theorems for optimization," *IEEE Trans. Evol. Comput.*, vol. 1, no. 1, pp. 67–82, Apr. 1997.

[24] M. Kermadi, V. J. Chin, S. Mekhilef, and Z. Salam, "A fast and accurate generalized analytical approach for PV arrays modeling under partial shading conditions," *Sol. Energy*, vol. 208, pp. 753–765, Oct. 2020.

[25] R. Abbassi, A. Abbassi, A. A. Heidari, and S. Mirjalili, "An efficient salp swarm-inspired algorithm for parameters identification of photovoltaic cell models," *Energy Convers. Manage.*, vol. 179, pp. 362–372, Jan. 2019.
[26] N. Barth, R. Jovanovic, S. Ahzi, and M. A. Khaleel, "Pv panel single and double diode models: Optimization of the parameters and temperature dependence," *Sol. Energy Mater. Sol. Cells*, vol. 148, pp. 87–98, Oct. 2016.
[27] D. Yousri, A. Fathy, H. Rezk, T. S. Babu, and M. R. Berber, "A reliable approach for modeling the photovoltaic system under partial shading conditions using three diode model and hybrid marine predators-slime mould algorithm," *Energy Convers. Manage.*, vol. 243, Oct. 2021, Art. no. 114269.
[28] M. Tripathy, M. Kumar, and P. Sadhu, "Photovoltaic system using Lambert W function-based technique," *Sol. Energy*, vol. 158, pp. 432–439, 2017.
[29] M. Ćalasan, S. H. A. Aleem, and A. F. Zobaa, "On the root mean square error (RMSE) calculation for parameter estimation of photovoltaic models: A novel exact analytical solution based on Lambert W function," *Energy Convers. Manage.*, vol. 210, Feb. 2020, Art. no. 112716.
[30] H. M. Ridha, "Parameters extraction of single and double diodes photovoltaic models using marine predators algorithm and Lambert W function," *Sol. Energy*, vol. 209, pp. 674–693, 2020.
[31] I. Ahmadianfar, A. A. Heidari, A. H. Gandomi, X. Chu, and H. Chen, "RUN beyond the metaphor: An efficient optimization algorithm based on Runge Kutta method," *Expert Syst. Appl.*, vol. 181, Feb. 2021, Art. no. 115079.
[32] L. Abualigah, D. Yousri, M. Abd Elaziz, A. A. Ewees, M. A. Al-qaness, and A. H. Gandomi, "Aquila optimizer: A novel meta-heuristic optimization algorithm," *Comput. Ind. Eng.*, vol. 157, Feb. 2021, Art. no. 107250.
[33] S. Yilmaz and S. Sen, "Electric fish optimization: A new heuristic algorithm inspired by electrolocation," *Neural Comput. Appl.*, vol. 32, no. 15, pp. 11543–11578, 2020.
[34] M. H. Sulaiman, Z. Mustaffa, M. M. Saari, and H. Daniyal, "Barnacles mating optimizer: A new bio-inspired algorithm for solving engineering optimization problems," *Eng. Appl. Artif. Intell.*, vol. 87, May 2020, Art. no. 103330.
[35] M. Braik, A. Sheta, and H. Al-Hiary, "A novel meta-heuristic search algorithm for solving optimization problems: Capuchin search algorithm," *Neural Comput. Appl.*, vol. 33, no. 7, pp. 2515–2547, Apr. 2021.
[36] D. Połap and M. Woźniak, "Red fox optimization algorithm," *Expert Syst. Appl.*, vol. 166, Jun. 2021, Art. no. 114107.
[37] J. Ma, T. O. Ting, K. L. Man, N. Zhang, S.-U. Guan, and P. W. H. Wong, "Parameter estimation of photovoltaic models via cuckoo search," *J. Appl. Math.*, vol. 2013, pp. 1–8, Jun. 2013.
[38] K. J. Yu, J. J. Liang, B. Y. Qu, Z. P. Cheng, and H. S. Wang, "Multiple learning backtracking search algorithm for estimating parameters of photovoltaic models," *Appl. Energy*, vol. 226, pp. 408–422, Sep. 2018.
[39] O. Hachana, K. E. Hemsas, G. M. Tina, and C. Ventura, "Comparison of different Metaheuristic algorithms for parameter identification of photovoltaic cell/module," *J. Renew. Sustain. Energy*, vol. 5, no. 5, Sep. 2013, Art. no. 053122.
[40] T. Kang, J. Yao, M. Jin, S. Yang, and T. Duong, "A novel improved cuckoo search algorithm for parameter estimation of photovoltaic (PV) models," *Energies*, vol. 11, no. 5, p. 1060, Apr. 2018.
[41] X. Gao, Y. Cui, J. Hu, G. Xu, Z. Wang, J. Qu, and H. Wang, "Parameter extraction of solar cell models using improved shuffled complex evolution algorithm," *Energy Convers. Manage.*, vol. 157, pp. 460–479, Feb. 2018.
[42] D. Yousri, S. B. Thanikanti, D. Allam, V. K. Ramachandaramurthy, and M. Eteiba, "Fractional chaotic ensemble particle swarm optimizer for identifying the single, double, and three diode photovoltaic models' parameters," *Energy*, vol. 195, Mar. 2020, Art. no. 116979.
[43] H. Wei, J. Cong, X. Lingyun, and S. Deyun, "Extracting solar cell model parameters based on chaos particle swarm algorithm," in *Proc. Int. Conf. Electr. Inf. Control Eng. (ICEICE)*, 2011, pp. 398–402.
[44] D. Yousri, D. Allam, M. Eteiba, and P. N. Suganthan, "Static and dynamic photovoltaic models' parameters identification using chaotic heterogeneous comprehensive learning particle swarm optimizer variants," *Energy Convers. Manage.*, vol. 182, pp. 546–563, Oct. 2019.
[45] K. Yu, X. Chen, X. Wang, and Z. Wang, "Parameters identification of photovoltaic models using self-adaptive teaching-learning-based optimization," *Energy Convers. Manage.*, vol. 145, pp. 233–246, Aug. 2017.
[46] A. M. Beigi and A. Maroosi, "Parameter identification for solar cells and module using a hybrid firefly and pattern search algorithms," *Sol. Energy*, vol. 171, no. 1, pp. 435–446, Sep. 2018.
[47] A. R. Jordehi, "Time varying acceleration coefficients particle swarm optimisation (tvacpso): A new optimisation algorithm for estimating parameters of PV cells and modules," *Energy Convers. Manage.*, vol. 129, pp. 262–274, Mar. 2016.
[48] J. A. Jervase, H. Bourdoucen, and A. Al-Lawati, "Solar cell parameter extraction using genetic algorithms," *Meas. Sci. Technol.*, vol. 12, no. 11, p. 1922, 2001.
[49] K. J. Yu, B. Y. Qu, C. T. Yue, S. L. Ge, X. Chen, and J. Liang, "A performance-guided JAYA algorithm for parameters identification of photovoltaic cell and module," *Appl. Energy*, vol. 237, no. 1, pp. 241–257, Mar. 2019.
[50] D. Oliva, M. A. El Aziz, and A. E. Hassanien, "Parameter estimation of photovoltaic cells using an improved chaotic whale optimization algorithm," *Appl. Energy*, vol. 200, pp. 141–154, Aug. 2017.
[51] A. R. Jordehi, "Gravitational search algorithm with linearly decreasing gravitational constant for parameter estimation of photovoltaic cells," in *Proc. Congr. Evol. Comput. (CEC)*, 2017, pp. 37–42.
[52] J. Ma, K. L. Man, S.-U. Guan, T. O. Ting, and P. W. H. Wong, "Parameter estimation of photovoltaic model via parallel particle swarm optimization algorithm," *Int. J. Energy Res.*, vol. 40, no. 3, pp. 343–352, Oct. 2016.
[53] X. Chen, K. Yu, W. Du, W. Zhao, and G. Liu, "Parameters identification of solar cell models using generalized oppositional teaching learning based optimization," *Energy*, vol. 99, pp. 170–180, Mar. 2016.
[54] N. F. A. Hamid, N. A. Rahim, and J. Selvaraj, "Solar cell parameters identification using hybrid nelder-mead and modified particle swarm optimization," *J. Renew. Sustain. Energy*, vol. 8, no. 1, Jan. 2016, Art. no. 015502.
[55] D. F. Alam, D. A. Yousri, and M. B. Eteiba, "Flower pollination algorithm based solar PV parameter estimation," *Energy Convers. Manage.*, vol. 101, no. 1, pp. 410–422, Sep. 2015.

DALIA YOUSRI received the B.Tech. (Hons.), M.Tech., and Ph.D. degrees from the Faculty of Engineering, Fayoum University, Egypt, in 2011, 2016, and 2020, respectively. She is currently working as a Lecturer at the Faculty of Engineering, Fayoum University. She has published refereed manuscripts in the fields of optimization algorithms, photovoltaic applications, fuel cell, chaotic systems, and fractional calculus with some topics. Acting as a Reviewer for various reputed journals, such as the IEEE Access, IET, *Energy Conversion and Management*, *Applied Soft Computing*, *International Journal of Electronics and Communications*, *Artificial Intelligence Review* (Springer), and *Neural Computing and Applications*. Her research interests include the modifications of optimization algorithms, modeling, and implementation of solar PV systems, fuel cell technologies, and fractional calculus topics.

MOHAMMED MUDHSH received the bachelor's and master's degrees in computer science from Basra University and the Ph.D. degree in computer science and technology from the Wuhan University of Technology, in 2017. In 2020, he joined the School of Information Engineering, Henan Institute of Science and Technology, as an Assistant Professor. His research interests include image processing, features extraction, handwriting recognition, and deep learning. In recent years, he has focused on optimization algorithm. He has collaborated actively with researches in several other disciplines of computer science.

YOMNA O. SHAKER received the B.Sc. degree (Hons.) from Fayoum University, Egypt, in 1998, and the M.Sc. and Ph.D. degrees from Cairo University, Cairo, Egypt, in 2003 and 2010, respectively. She was a Visiting Scholar at American University, Sharjah, from 2012 to 2015. She is currently an Assistant Professor with the Department of Electrical Engineering, University of Science and Technology of Fujairah (USTF), United Arab Emirates, and Fayoum University (in leave). Her research and teaching interests include high voltage equipment electrical machines and renewable energy.

LAITH ABUALIGAH received the degree in computer information system and the master's degree in computer science from Al Albayt University, Jordan, in 2011 and 2014, respectively, and the Ph.D. degree from the School of Computer Science, Universiti Sains Malaysia (USM), Malaysia, in 2018. He is currently an Assistant Professor at the Computer Science Department, Amman Arab University, Jordan. He has published more than 70 journal articles and books, which collectively have been cited more than 2000 times (H-index = 23). His main research interests include bio-inspired computing, artificial intelligence, metaheuristic modeling, and optimization algorithms, evolutionary computations, information retrieval, feature selection, combinatorial problems, optimization, advanced machine learning, big data, and natural language processing.

ELSAYED TAG-ELDIN was the Dean of the Faculty of Engineering, Cairo University, where he achieved many unique signs of progress in both academia and research on the impact of emerging technologies in electrical engineering. He is currently with Future University, Egypt, on leave from Cairo University after nearly 30 years of service to the Faculty of Engineering, Cairo University. He was a PI of several nationally and internationally funded projects. He has many publications in highly refereed international journals and specialized conferences in the applications of artificial intelligence on protection of electrical power networks. In addition, he is in the editorial boards of several *International Journal of Power and Energy Systems*.

MOHAMED ABD ELAZIZ received the B.S. and M.S. degrees in computer science and the Ph.D. degree in mathematics and computer science from Zagazig University, Egypt, in 2008, 2011, and 2014, respectively. From 2008 to 2011, he was an Assistant Lecturer with the Department of Computer Science. He is currently an Associate Professor at Zagazig University. He is the author of more than 200 articles. He is one of the 2% influential scholars, which depicts the 100,000 top-scientists in the world. His research interests include metaheuristic technique, security IoT, cloud computing machine learning, signal processing, image processing, and evolutionary algorithms.

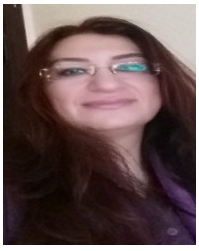

DALIA ALLAM received the B.Sc., M.Sc., and Ph.D. degrees in electrical power engineering from Cairo University, Egypt. She was certified as a Siemens Trainer in several automation subjects. She was an Ex-Manager of the Automatic Control Unit, Fayoum University, Egypt, where she is currently an Associate Professor with the Electrical Engineering Department. She has many publications in highly refereed international journals. Her research interests include applications of AI and SI in electrical power engineering, renewable energy, power quality, smart relays and digital protection systems, and automation and process control. She is also a reviewer for many international journals.